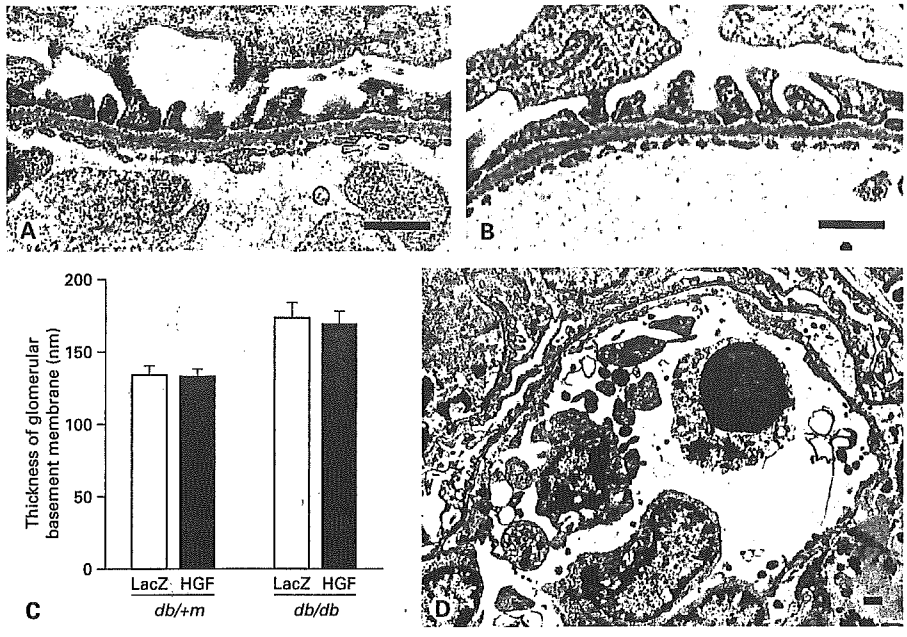

Fig. 5. Electron microphotographs of glomerular lesions observed in 24-week-old *db/db* mice. Glomerular basement membrane in the LacZ-treated (**A**) and HGF-treated *db/db* mouse (**B**). **C** Comparison of thickness of glomerular basement membrane between the LacZ- and HGF-treated mice. **D** Apoptosis of a glomerular capillary endothelial cell observed in the LacZ-treated *db/db* mouse. Bars = 1 μm.

as in the *db/db* mice, the gene therapy significantly affected the renal pathological parameters. The HGF-treated *db/db* mice showed significantly greater glomerular area and glomerular cell number than the LacZ-treated *db/db* mice (fig. 3, 4). Hypocellular, sclerotic lesions compatible with diabetic glomerulosclerosis were observed in glomeruli of the both groups under a light microscope, but its extent appeared smaller in the HGF-treated group. The glomerular sclerotic index calculated as the percent area of PAS-positive area in the glomerulus was reciprocally smaller in the HGF-treated mice. In addition, the percent area of fibrosis assessed by Sirius red stain was smaller in both glomerular and tubular areas.

Ultrastructural morphometry revealed that the thickness of the glomerular basement membrane was similar between the LacZ- (173 ± 4 nm) and HGF-treated (168 ± 4 nm) *db/db* mice, which were greater than those of *db/+m* mice (fig. 4).

Proliferation and Apoptosis

To seek the mechanisms for the increased glomerular cell population by the HGF treatment in the *db/db* mice, we next investigated proliferating activity and apoptosis of kidneys of the *db/db* mice. PCNA-positive cells were observed in glomeruli and tubules of both LacZ- and HGF-treated mice (fig. 4). The incidence of the PCNA-positive cells in glomeruli and that in tubules of the HGF-treated mice were similar between the groups (fig. 5). TUNEL positivity was noted in glomerular and tubular cells in both groups although in low incidences (fig. 4), and electron microscopy demonstrated apoptotic cells (fig. 6). The HGF treatment resulted in a significant reduction in the incidence of TUNEL-positive cells in both glomeruli and tubules, compared with the LacZ treatment (fig. 5).

According to double immunohistochemistry for Flk-1 with PCNA or TUNEL (fig. 4), the HGF gene therapy resulted in no significant change in the proliferation of glomerular endothelial cells and tubular epithelial cells, although a significant decrease in their apoptosis was noted (fig. 5).

Expression of TGF-β1

Consistent with the previous report [29], expression of TGF-β1 in the kidney was greater in the *db/db* mice than in the *db/+m* mice (data not shown). It was found that expression of TGF-β1 in the kidney was significantly reduced in the HGF-treated *db/db* mice, compared with the LacZ-treated ones (fig. 7).

Survival Study

Finally, we examined the effect of HGF gene therapy on the survival of *db/db* mice. Thirteen of 15 *db/db* mice (87%) treated with HGF gene survived over the subsequent 25 weeks, whereas only 7 of 15 *db/db* mice (47%)

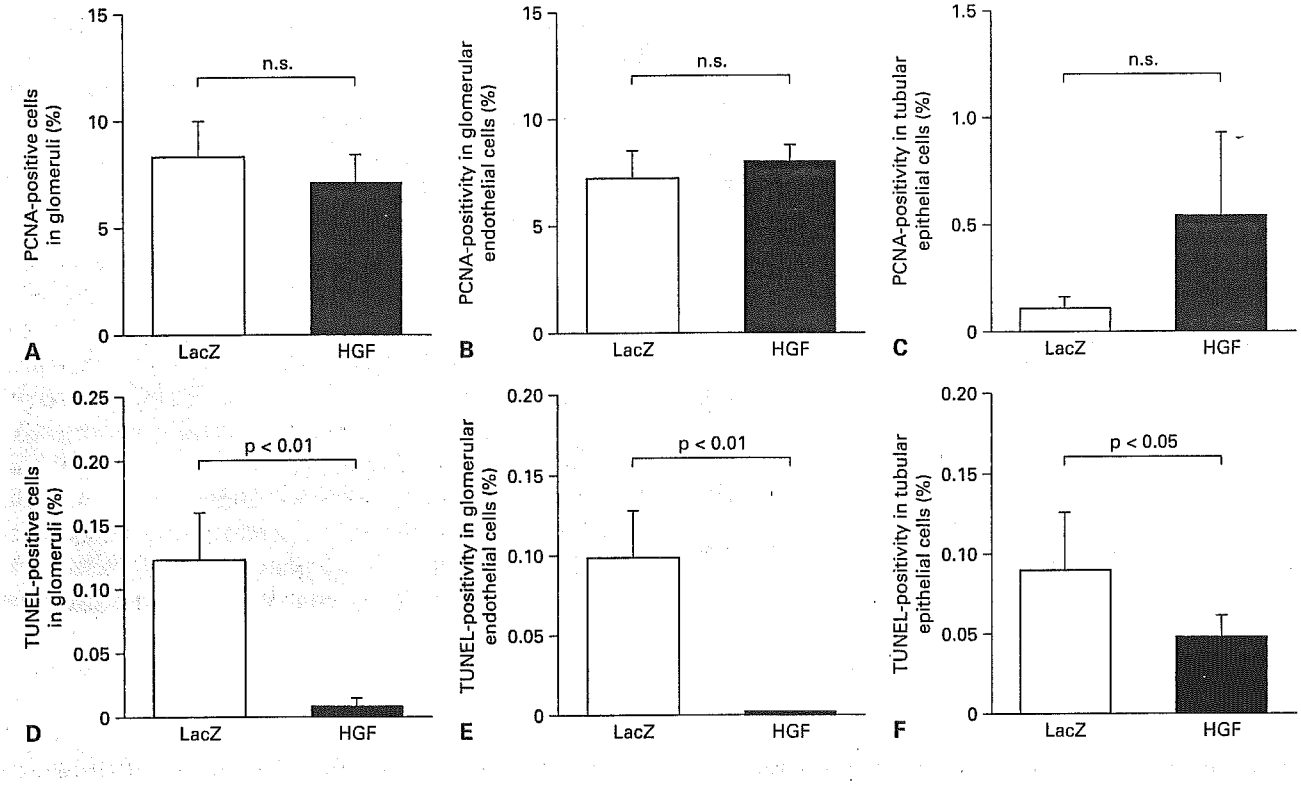

Fig. 6. Quantitative morphometry of PCNA- (**A–C**) or TUNEL-positive (**D–F**) cells in renal glomeruli or tubules of *db/db* mice treated with LacZ or HGF gene. Percent PCNA-positive cells in renal glomeruli (**A**) and in tubules (**C**). Percent TUNEL-positive cells in glomeruli (**D**) and in tubules (**F**). Percent PCNA-positive (**B**) or percent TUNEL-positive (E) glomerular endothelial cells assessed in double immunohistochemical preparations.

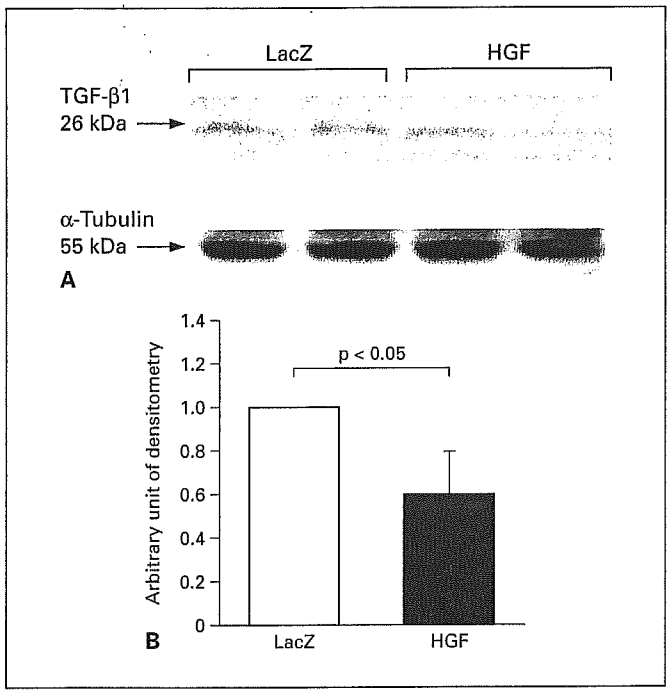

Fig. 7. Western blot for TGF-β1 in kidneys (**A**), and its densitometric analysis (**B**). Y-axis indicates arbitrary unit of densities.

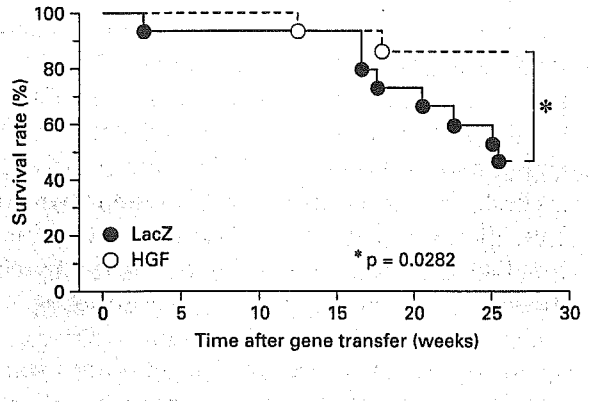

Fig. 8. Survival curve for the HGF- and LacZ-treated *db/db* mice. The mice were treated with HGF gene (n = 15) or LacZ gene (n = 15) at the age of 12 weeks and followed for 25 weeks. There was a significant difference (p = 0.0282) in the survival rate between the groups.

treated with the LacZ gene survived within the interval. Comparison of survival curves by the Kaplan and Meier method showed a significant difference between the HGF- and LacZ-treated groups (log-rank 4.814, p = 0.0282) (fig. 8).

Discussion

In general, diabetic nephropathy progresses from the glomerular hyperfiltration stage into the glomerular sclerotic stage with reduced glomerular filtration [30–32]. The diabetic *db/db* mice displayed far greater urine volume and Ccr than the nondiabetic *db/+m* mice, suggesting that the *db/db* mice at the beginning of the experiment were already suffering from the glomerular hyperfiltration stage of diabetic nephropathy. The *db/db* mice treated with the LacZ gene in the present study showed this progression into the glomerular sclerotic stage during the observation period, i.e. progressive reduction in urine volume and Ccr. However, the present study revealed that the HGF gene therapy markedly prevented this progression. Pathologically, the HGF gene therapy resulted in a significant prevention of formation of glomerular sclerotic lesions and of glomerular and tubular fibrosis that was marked in the LacZ-treated *db/db* mice. The glomerular cell population of the HGF-treated mice was also significantly greater than that of the LacZ-treated mice. Overall, it is apparent that the HGF gene therapy slowed down the progressive deterioration in functional and pathological aspects of diabetic nephropathy in the *db/db* mice. More importantly, this therapy improved survival of these mice. It was apparent that the beneficial effect of HGF on diabetic nephropathy was irrelevant to glucose metabolism since levels of blood glucose and HbA1c were similar between the HGF-untreated and -treated *db/db* mice. The present study also confirmed that such effects of the HGF gene therapy were not observed in nondiabetic *db/+m* mice.

The glomerular cell population, endothelial cell population in particular, was significantly greater in the HGF gene-treated *db/db* mice. According to immunohistochemistry for Flk-1 combined with TUNEL assay, the HGF gene therapy suppressed glomerular endothelial cell and tubular epithelial cell apoptosis in *db/db* mice. Thus, the present study demonstrated an anti-apoptotic effect of HGF on those cells. In particular, preservation of the glomerular endothelial cell population by such mechanism might have greatly contributed to the functional maintenance of glomerular filtration, because the endothelial cells secure the area for glomerular filtration. Although the thickness of the glomerular basement membrane was also an important regulator of glomerular filtration, the ultrastructural morphometry of the present study did not confirm this contribution.

Previous studies reported an anti-fibrotic effect of HGF in the renal tubulointerstitium of animals with chronic renal diseases including experimentally induced diabetic nephropathy [17–20]. Consistent with these findings, the present HGF gene therapy resulted in suppression of fibrosis not only in the glomerulus but also in the tubulointerstitium of the *db/db* mice. Moreover, similar to the capillary endothelial cells, tubular epithelial cells showed decreased apoptosis. Thus, HGF exerted beneficial effects by affecting both glomerular and tubulointerstitial lesions of diabetic nephropathy. The HGF gene therapy resulted in a smaller glomerular sclerotic index and a more reduced fibrotic area in glomeruli of diabetic nephropathy, compared with the LacZ gene treatment. Thus, the HGF gene therapy alleviated the progression to glomerular obsolescence in diabetic nephropathy through a reduction in the mesangial matrix and fibrosis and also through maintenance of the glomerular cell component, endothelial cells in particular. An opposite effect of HGF against TGF-β was reported previously [15, 33, 34]. In the present study, the Western blot analysis actually demonstrated greatly attenuated expression of TGF-β1 in the HGF-treated kidneys of *db/db* mice. Since TGF-β, in addition to platelet-derived growth factor (PDGF), accelerates transformation of mesangial cells into myofibroblasts

that potentially produce collagen fibers [35, 36], such an anti-TGF-β effect of HGF may be important for attenuation of glomerulosclerosis in diabetic nephropathy. Alternatively, as Mizuno et al. [17] previously suggested, an endothelial protective effect of HGF may play an important role for the prevention of glomerulosclerosis.

Mizuno et al. [19] recently reported beneficial effect of injection of recombinant human HGF on streptozotocin-induced diabetic nephropathy in mice. Although our findings were mostly consistent with theirs, there are some discrepancies in some aspects. They found that HGF treatment reduced glomerular area and suppressed glomerular hyperfiltration, which were opposite to our findings. It may be most likely that the discrepancy was caused by the difference of animal models with different stage and progression of diabetic nephropathy; our model might be at the later stage than that of Mizuno et al. as it was already at the hyperfiltration stage at the beginning of the experiments. Laping et al. [37] reported that diabetic nephropathy in *db/db* mice was aggravated by an HGF supplement. However, the dose of HGF used in the study seemed to be too low to attain and sustain physiological HGF level as Mizuno et al. [19] pointed out. In our study, the plasma HGF levels were considered sufficiently high because the level was greater at any time point measured than that produced by the plasmid DNA injection in another study [38], which effectively prevented progression of liver cirrhosis in an animal model. The way in which the very low dose of HGF has different effects awaits results from additional studies.

The HGF gene therapy on diabetic nephropathy indeed delayed the disease progression, but this suggests that the therapy made the mice stay longer in the glomerular hyperfiltration phase of diabetic nephropathy where albuminuria continues. Although no significant reduction of the serum albumin level was observed in the HGF-treated group, a longer follow-up of the animals may be needed to check what such continuous albuminuria would yield. Thus, the examination of cause of death of the HGF-treated *db/db* mice may be of importance and such an investigation is warranted in future. Nevertheless, in the present study, the survival rate was improved by the HGF gene treatment. There has been no clinically effective treatment for the pathological condition of patients with diabetic nephropathy. Even a strict control of hyperglycemia does not necessarily guarantee deceleration of disease progression [32], and many patients have to enter chronic dialysis programs with renal failure. Effective HGF supply would delay the start of the dialysis program, and it is suggested that it would be one of the promising candidates for preventing, or at least slowing down the progression of clinical and pathophysiological manifestations of diabetic nephropathy.

Acknowledgements

We thank Akiko Tsujimoto, Hatsue Ohshika, Kazuko Gotoh, Toshie Ohtsubo, and the staff of Kyoto Women's University (Kaori Abe, Keiko Uozu, Kazumi Ohara, Hitomi Takagaki, Machiko Mizutani, and Miyuki Morikawa) for technical assistance.

References

1 Ritz E, Orth SR: Nephropathy in patients with type 2 diabetes mellitus. N Engl J Med 1999; 341:1127–1133.
2 Woodrow D, Moss J, Shore I, Spiro RG: Diabetic glomerulosclerosis: Immunogold ultrastructural studies on the glomerular distribution of type IV collagen and heparan sulphate proteoglycan. J Pathol 1992;167:49–58.
3 Mohan PS, Carter WG, Spiro RG: Occurrence of type VI collagen in extracellular matrix of renal glomeruli and its increase in diabetes. Diabetes 1990;39:31–37.
4 Border WA, Noble NA: Transforming growth factor-β in tissue fibrosis. N Engl J Med 1994; 331:1286–1292.
5 Hong SW, Isono M, Chen S, Iglesias-De La Cruz MC, Han DC, Ziyadeh FN: Increased glomerular and tubular expression of transforming growth factor-β1, its type II receptor, and activation of the Smad signaling pathway in the db/db mouse. Am J Pathol 2001;158: 1653–1663.
6 Ishii N, Ogawa Z, Suzuki K, Numakami K, Saruta T, Itoh H: Glucose loading induces DNA fragmentation in rat proximal tubular cells. Metabolism 1996;45:1348–1353.
7 Ortiz A, Ziyadeh FN, Neilson EG: Expression of apoptosis-regulatory genes in renal proximal tubular epithelial cells exposed to high ambient glucose and in diabetic kidneys. J Invest Med 1997;45:50–56.
8 Murata I, Takemura G, Asano K, Sano H, Fujisawa K, Kagawa T, Baba K, Maruyama R, Minatoguchi S, Fujiwara T, Fujiwara H: Apoptotic cell loss following cell proliferation in renal glomeruli of Otsuka Long-Evans Tokushima fatty rats, a model of human type 2 diabetes. Am J Nephrol 2002;22:587–595.
9 Nakamura T, Nawa K, Ichihara A: Partial purification and characterization of hepatocyte growth factor from serum of hepatectomized rats. Biochem Biophys Res Commun 1984; 122:1450–1459.
10 Nakamura T, Nishizawa T, Hagiya M, Seki T, Shimonishi M, Sugimura A, Tashiro K, Shimizu S: Molecular cloning and expression of human hepatocyte growth factor. Nature 1989; 342:440–443.
11 Birchmeier C, Gherardi E: Developmental roles of HGF/SF and its receptor, the c-Met tyrosine kinase. Trends Cell Biol 1998;8:404–410.
12 Kosai K, Matsumoto K, Funakoshi H, Nakamura T: Hepatocyte growth factor prevents endotoxin-induced lethal hepatic failure in mice. Hepatology 1999;30:151–159.
13 Xiao GH, Jeffers M, Bellacosa A, Mitsuuchi Y, Vande Woude GF, Testa JR: Anti-apoptotic signaling by hepatocyte growth factor/Met via the phosphatidylinositol 3-kinase/Akt and mitogen-activated protein kinase pathways. Proc Natl Acad Sci USA 2001;98:247–252.

14 Nakagami H, Morishita R, Yamamoto K, Taniyama Y, Aoki M, Matsumoto K, Nakamura T, Kaneda Y, Horiuchi M, Ogihara T: Mitogenic and antiapoptotic actions of hepatocyte growth factor through ERK, STAT3, and AKT in endothelial cells. Hypertension 2001;37:581–586.
15 Mizuno S, Matsumoto K, Kurosawa T, Mizuno-Horikawa Y, Nakamura T: Reciprocal balance of hepatocyte growth factor and transforming growth factor-beta 1 in renal fibrosis in mice. Kidney Int 2000;57:937–948.
16 Matsumoto K, Nakamura T: Hepatocyte growth factor: renotropic role and potential therapeutics for renal diseases. Kidney Int 2001;59:2023–2038.
17 Mizuno S, Kurosawa T, Matsumoto K, Mizuno-Horikawa Y, Okamoto M, Nakamura T: Hepatocyte growth factor prevents renal fibrosis and dysfunction in a mouse model of chronic renal disease. J Clin Invest 1998;101:1827–1834.
18 Mizuno S, Matsumoto K, Nakamura T: Hepatocyte growth factor suppresses interstitial fibrosis in a mouse model of obstructive nephropathy. Kidney Int 2001;59:1304–1314.
19 Mizuno S, Nakamura T: Suppressions of chronic glomerular injuries and TGF-beta 1 production by HGF in attenuation of murine diabetic nephropathy. Am J Physiol 2004;286: F134–F143.
20 Cruzado JM, Lloberas N, Torras J, Riera M, Fillat C, Herrero-Fresneda I, Aran JM, Alperovich G, Vidal A, Grinyo JM: Regression of advanced diabetic nephropathy by hepatocyte growth factor gene therapy in rats. Diabetes 2004;53:1119–1127.
21 Hummel KP, Dickie MM, Coleman DL: Diabetes, a new mutation in the mouse. Science 1996;153:1127–1128.
22 Like AA, Lavine RL, Poffenbarger PL, Chick WL: Studies in the diabetic mutant mice. Diabetologia 1974;10:607–610.
23 Cohen MP, Clements RS, Hud E, Cohen JA, Ziyadeh FN: Evolution of renal function abnormalities in the db/db mouse that parallels the development of human diabetic nephropathy. Exp Nephrol 1996;4:166–171.
24 Mizuguchi H, Kay AM: A simple method for constructing E1- and E1/E4-deleted recombinant adenoviral vectors. Hum Gen Ther 1999; 10 2013–2017.
25 Chen SH, Chen XH, Wang Y, Kosai K, Finegold MJ, Rich SS, Woo SL: Combination gene therapy for liver metastasis of colon carcinoma in vivo. Proc Natl Acad Sci USA 1995;92: 2577–2581.
26 Junqueira LC, Bignolas G, Brentani RR: Red sirius staining plus polarizing microscopy: a specific method for collagen detection in tissue sections. Histochem J 1979;79:445–447.
27 Matsumae T, Jimi S, Uesugi N, Takebayashi S, Naito S: Clinical and morphometrical interrelationships in patients with overt nephropathy induced by non-insulin-dependent diabetes mellitus: a light- and electron-microscopy study. Nephron 1999;81:41–48.
28 Li Y, Takemura G, Kosai K, Yuge K, Nagano S, Esaki M, Goto K, Takahashi T, Hayakawa K, Koda M, Kawase Y, Maruyama R, Okada H, Minatoguchi S, Mizuguchi H, Fujiwara T, Fujiwara H: Postinfarction treatment with an adenoviral vector expressing hepatocyte growth factor relieves chronic left ventricular remodeling and dysfunction in mice. Circulation 2003;107:2499–2506.
29 Ziyadeh FN, Hoffman BB, Han D-C, Iglesias-de la Cruz MC, Hong S-w, Isono M, Chen S, McGowan TA, Sharma K: Long-term prevention of renal insufficiency, excess matrix gene expression, and glomerular mesangial matrix expansion by treatment with monoclonal anti-transforming growth factor-β antibody in db/db diabetic mice. Proc Natl Acad Sci USA 2000;97:8015–8020.
30 Mauer SM, Steffes MW, Ellis EN, Sutherland DE, Brown DM, Goetz FC: Structural-functional relationships in diabetic nephropathy. J Clin Invest 1984;74:1143–1155.
31 Fabre J, Balant LP, Dayer PG, Fox HM, Vernet AT: The kidney in maturity onset diabetes mellitus: a clinical study of 510 patients. Kidney Int 1982;21:730–738.
32 Viberti G, Wiseman MJ, Pinto JR, Messent J: Diabetic Nephropathy; in Kahn CR, Weir GC (eds): Joslin's Diabetes mellitus, ed 13. Malvern, Lea & Febiger, 1997, pp 691–737.
33 Yasuda H, Imai E, Shiota A, Fujise N, Morinaga T, Higashio K: Antifibrogenic effect of a deletion variant of hepatocyte growth factor on liver fibrosis in rats. Hepatology 1996;24:636–642.
34 Taniyama Y, Morishita R, Nakagami H, Moriguchi A, Sakonjo H, Shokei-Kim, Matsumoto K, Nakamura T, Higaki J, Ogihara T: Potential contribution of a novel antifibrotic factor, hepatocyte growth factor, to prevention of myocardial fibrosis by angiotensin II blockade in cardiomyopathic hamsters. Circulation 2000; 102:246–252.
35 Tang WW, Ulich TR, Lacey DL, Hill DC, Qi M, Kaufman SA, Van GY, Tarpley JE, Yee JS: Platelet-derived growth factor-BB induces renal tubulointerstitial myofibroblast formation and tubulointerstitial fibrosis. Am J Pathol 1996:148:1169–1180.
36 el Nahas AM, Muchaneta-Kubara EC, Zhang G, Adam A, Goumenos D: Phenotypic modulation of renal cells during experimental and clinical renal scarring. Kidney Int 1996;54: S23–S27.
37 Laping NJ, Olson BA, Ho T, Ziyadeh FN, Albrightson CR: Hepatocyte growth factor: a regulator of extracellular matrix genes in mouse mesangial cells. Biochem Pharmacol 2000;59: 847–853.
38 Ueki T, Kaneda Y, Tsutsui H, Nakanishi K, Sawa Y, Morishita R, Matsumoto K, Nakamura T, Takahashi H, Okamoto E, Fujimoto J: Hepatocyte growth factor gene therapy of liver cirrhosis in rats. Nat Med 1999;5:226–230.

Laboratory Investigation (2005) 1–12

www.laboratoryinvestigation.org

Local overexpression of HB-EGF exacerbates remodeling following myocardial infarction by activating noncardiomyocytes

Hiroaki Ushikoshi[1,2], Tomoyuki Takahashi[1,4,5], Xuehai Chen[2], Ngin Cin Khai[1,2], Masayasu Esaki[1,2], Kazuko Goto[1,2], Genzou Takemura[2], Rumi Maruyama[2], Shinya Minatoguchi[2], Takako Fujiwara[3], Satoshi Nagano[1,4], Kentaro Yuge[1], Takao Kawai[1,2], Yoshiteru Murofushi[1,4], Hisayoshi Fujiwara[2] and Ken-ichiro Kosai[1,4,6]

[1]*Department of Gene Therapy and Regenerative Medicine, Gifu University School of Medicine, Gifu, Japan;* [2]*Department of Cardiology, Respirology and Nephrology, Regeneration & Advanced Medical Science, Gifu University Graduate School of Medicine, Gifu, Japan;* [3]*Department of Food Science, Kyoto Women's University, Kyoto, Japan;* [4]*Division of Gene Therapy and Regenerative Medicine, Cognitive and Molecular Research Institute of Brain Diseases, Kurume University, Kurume, Japan;* [5]*Department of Advanced Therapeutics and Regenerative Medicine, Kurume University School of Medicine, Kurume, Japan and* [6]*Department of Pediatrics and Child Health, Kurume University School of Medicine, Kurume, Japan*

Insulin-like growth factor (IGF), hepatocyte growth factor (HGF), and heparin-binding epidermal growth factor-like growth factor (HB-EGF) are cardiogenic and cardiohypertrophic growth factors. Although the therapeutic effects of IGF and HGF have been well demonstrated in injured hearts, it is uncertain whether natural upregulation of HB-EGF after myocardial infarction (MI) plays a beneficial or pathological role in the process of remodeling. To answer this question, we conducted adenoviral HB-EGF gene transduction in *in vitro* and *in vivo* injured heart models, allowing us to highlight and explore the HB-EGF-induced phenotypes. Overexpressed HB-EGF had no cytoprotective or additive death-inducible effect on Fas-induced apoptosis or oxidative stress injury in primary cultured mouse cardiomyocytes, although it significantly induced hypertrophy of cardiomyocytes and proliferation of cardiac fibroblasts. Locally overexpressed HB-EGF in the MI border area in rabbit hearts did not improve cardiac function or exhibit an angiogenic effect, and instead exacerbated remodeling at the subacute and chronic stages post-MI. Namely, it elevated the levels of apoptosis, fibrosis, and the accumulation of myofibroblasts and macrophages in the MI area, in addition to inducing left ventricular hypertrophy. Thus, upregulated HB-EGF plays a pathophysiological role in injured hearts in contrast to the therapeutic roles of IGF and HGF. These results imply that regulation of HB-EGF may be a therapeutic target for treating cardiac hypertrophy and fibrosis.
Laboratory Investigation advance online publication, 25 April 2005; doi:10.1038/labinvest.3700282

Keywords: apoptosis; gene transfer; growth factor; myocardial infarction; remodeling

Heparin-binding epidermal growth factor-like growth factor (HB-EGF), a member of the EGF-family of growth factors, is synthesized as a type I transmembrane protein (proHB-EGF).[1] Membrane-bound proHB-EGF is cleaved at its juxtamembrane domain by a specific metalloproteinase, resulting in shedding of soluble HB-EGF.[2] Whereas soluble HB-EGF is a potent mitogen for a number of cell types, including vascular smooth muscle cells, fibroblasts, keratinocytes, and hepatocytes,[3–5] the activity of proHB-EGF may be mitogenic or growth inhibitory depending on cell type.[6]

HB-EGF has been implicated in a number of physiological and pathological processes. HB-EGF may play a role in the development of atherosclerosis resulting from smooth muscle cell hyperplasia,[4,7,8] pulmonary hypertension, and oncogenic transformation.[9,10] In contrast, HB-EGF is

Correspondence: Dr K Kosai, MD, PhD, Division of Gene Therapy and Regenerative Medicine, Cognitive and Molecular Research Institute of Brain Diseases, Kurume University, 67 Asahi-machi, Kurume 830-0011, Japan.
E-mail: kosai@med.kurume-u.ac.jp
Received 27 November 2004; revised 9 March 2005; accepted 15 March 2005; published online 25 April 2005

therapeutic for the skin,[11,12] kidney,[13,14] liver, and small intestine.[3,5,15,16] HB-EGF is markedly upregulated during the acute phase of injury and plays an essential role in epithelial cell repair, proliferation and regeneration in these organs.[5,11,13,15,17] Further direct evidence of therapeutic benefit was provided by studies of administration of recombinant HB-EGF in animal ischemic disease models.[16] Thus, HB-EGF plays a number of physiological roles, and its effects are diverse and even opposing in nature depending on the tissues examined.

It has been observed that HB-EGF-null mice develop severe heart failure associated with dilated ventricular chambers, diminished cardiac function, and grossly enlarged cardiac valves,[18,19] indicating that HB-EGF is an essential cardiogenic factor. HB-EGF is found in the adult heart under normal physiological conditions,[20] and the HB-EGF and/or EGF receptor (EGFR) families are further upregulated under pathological conditions such as cardiac hypertrophy[21] or myocardial infarction (MI).[22,23] Together with the recent finding that shedding of proHB-EGF results in cardiac hypertrophy,[24] it has recently been suggested that HB–EGF-induced cardiomyocyte hypertrophy plays a central role in hypertensive heart disease.[24,25] However, several previous studies demonstrated that overexpression of hepatocyte growth factor (HGF) and insulin-like growth factor (IGF), which are also cardiogenic growth factors, significantly induced cardiac hypertrophy but had potent therapeutic rather than pathologic effects in injured hearts, including those damaged by MI.[26–29] This led us to question whether HB-EGF might also possess therapeutic activity in the injured heart. Intriguingly, were HB-EGF to prove pathogenic, it could be the result of a secondary biological effect of this molecule separate from its promotion of hypertrophy. Thus, we endeavored to settle the questions raised by these conflicting reports in the most direct way possible, through targeted overexpression of HB-EGF in heart lesions.

One obvious approach by which to overexpress a target gene and explore the resulting effects would be to use transgenic mouse (TgM) technology, currently one of the most powerful approaches to elucidate directly the physiological and pathological roles of a gene of interest. In the present study, we opted instead to use an adenoviral gene transduction strategy, which allowed us to answer the same biological question while at the same time enabling a first assessment of the use of HB-EGF in gene therapy. Additionally, the use of an adenoviral vector allowed for greater spatial and temporal control of HB-EGF expression compared with the TgM approach, as persistent overexpression of the transgene (from the embryonic stage and before the onset of a disorder) may have produced data artefacts. Previous studies demonstrated that the expression of HB-EGF and EGFR family mRNAs was significantly increased around MI lesions.[22,23] In this context, adenoviral HB-EGF gene transduction around the MI area following onset of MI may serve to highlight the effect of HB-EGF on both cardiomyocytes and noncardiomyocytes following MI, offering a means to elucidate the role of this intriguing molecule in the development of heart disease.

Materials and methods

Recombinant Adenoviral Vectors

Replication-defective recombinant adenoviral vectors (Ads), Ad.HB-EGF and Ad.LacZ, which express HB-EGF or LacZ gene under the transcriptional control of a Rous sarcoma virus long-terminal repeat, were constructed as described previously.[27,30,31] All Ads were amplified in 293 cells, purified twice on CsCl gradients, and desalted.[27,30,31]

Injury Models in Primary Cultured Cardiomyocytes and Cardiac Fibroblasts

Cardiomyocytes and cardiac fibroblasts were isolated from 1-day-old neonatal Balb/c mice as previously reported.[32] The cardiomyoctes were incubated in Dulbecco's modified Eagle's medium (D-MEM, Sigma Chemical Co., St Louis, MO, USA) containing 5% fetal bovine serum (Sigma Chemical Co.) at 37°C for 24 h, and subsequently infected with Ads at various multiplicities of infection (MOI), followed by incubation in serum-free D-MEM for 48 h. In injury models of apoptosis and oxidative stress, cells were incubated with either 1 μg/ml agonistic anti-Fas antibody[33] (Jo2, Beckton-Dickinsion Biosciences, San Jose, CA, USA) with 0.05 μg/ml actinomycin D (Sigma Chemical Co.) for 24 h, or with 100 μM H_2O_2 (Wako Pure Chemical Industry, Osaka, Japan) for 1 h as previously described.[34,35] Cell viability was determined by WST-8 assay (Dojindo, Kumamoto, Japan) in accordance with the manufacturer's protocol 24 h after the induction of cell death.

For proliferation assays, cardiac fibroblasts were incubated in D-MEM supplemented with 5% fetal bovine serum, and were used following three or four passages. The purity of these cultures was >95% cardiac fibroblasts as confirmed by vimentin-positive, desmin-negative and α-smooth muscle actin-negative stainings as previously described.[36] WST-8 assay was performed at 24, 48 and 72 h after infection with Ads or addition of recombinant human HB-EGF (R&D Systems Inc., Minneapolis, MN, USA).

Immunocytochemistry and Analysis of Primary Cultured Cardiomyocytes

At 24 h following adenoviral infection at MOI 30, primary cultured cardiomyocytes were fixed in 4% paraformaldehyde, permeabilized with 0.05%

Triton-X and stained with primary goat anti-human HB-EGF antibody (R&D Systems Inc.), secondary donkey anti-goat IgG Alexa 488 antibody (Molecular Probes, Inc., Eugene, OR, USA), rhodamine phalloidin (Molecular Probes, Inc.) and Hoechst 33342 (Molecular Probes, Inc.). Digital images captured using a laser-confocal microscope system (LSM510, Carl Zeiss, Oberkochen, Germany) were employed for morphometric and quantitative analyses using Adobe Photoshop 7.0 software (Adobe Systems Inc., San Jose, CA, USA).

Animal Studies

Male Japanese white rabbits weighing 2–2.5 kg underwent a 30-min occlusion of the left coronary artery, followed by reperfusion, in order to generate MI as previously described.[37] Ad.HB-EGF or control Ad.LacZ (1×10^{11} viral particles) (each group, $n=16$) was directly injected into the border area between the risk and the intact areas at the time of reperfusion. Echocardiograms were recorded just before and 2 or 4 weeks after generation of MI. The rabbits were killed either 2 or 4 weeks later (each, $n=8$) and the hearts were collected, weighed, and then processed to obtain histological sections. In the sham control group ($n=4$), the chests of the rabbits were opened and closed under anesthesia without occlusion of the coronary artery or adenoviral injection, and echocardiograms and histological analyses were performed 2 or 4 weeks later. All animal studies were performed in accordance with the guidelines of the National Institute of Health as dictated by the Animal Care Facility at the Gifu University School of Medicine.

Adenoviral Gene Transduction Efficiencies and X-Gal Staining

The efficiency of *in vitro* and *in vivo* adenoviral gene transduction was analyzed by Ad.LacZ infection and X-gal staining, as previously described.[27,30,31]

Pathological Examination in Animal Experiments

The estimation of the risk and MI areas has been described previously.[37] Briefly, the coronary branch in the excised heart was reoccluded and 4% Evans blue dye (Sigma Chemical Co.) was injected via the aorta to determine the risk area. The LV was sectioned into seven slices parallel to the atrioventricular ring. Each slice was incubated in 1% solution of triphenyl tetrazolium chloride (TTC) to visualize the infarct area.

For histological analysis, the heart was fixed in 10% formalin and embedded in paraffin, and 4-μm sections were stained with hematoxylin and eosin (H–E) or Masson's trichrome for regular or fibrotic estimation, respectively. The sizes of individual cardiomyocytes were measured using the LUZEX F system (Nireco, Kyoto, Japan). Apoptotic cells were detected under light microscopy by terminal deoxynucleotidyl transferase-mediated deoxyuridine triphosphate biotin nick end labeling (TUNEL) assay (ApopTag kit, Intergen Co., Purchase, NY, USA) in accordance with the manufacturer's protocol. The immunohistochemical staining for proliferating cells, α-smooth muscle actin (SMA-positive cells), rabbit macrophages and vascular endothelial cells were carried out with anti-Ki-67 (MIB-1, Dako), anti-SMA (1A4, Dako), anti-RAM11 (Dako) and anti-CD31 (JC/70A, Dako) antibody, respectively, as described previously.[37] For fluorescent immunohistochemistry and TUNEL assay, 6-μm frozen sections were fixed in 4% paraformaldehyde and stained using a fluorescein-FragEL DNA fragmentation detection kit (Oncogene Research Products, San Diego, CA, USA) together with individual antibodies, according to the manufacturer's instructions.

Statistical Analysis

Data are represented as means $\pm$ standard error of the mean. Statistical significance was determined using Student's *t*-test. One-way ANOVA was used in multiple comparisons. $P<0.05$ was considered to be statistically significant. All statistical analysis was performed with StatView software (SAS Institute Inc., Cary, NC, USA).

Results

Adenoviral Gene Transduction Efficiency *In Vitro*

The adenoviral constructs demonstrated high infectivity in primary cultured mouse cardiomyocytes; infection of cardiomyocytes with Ad.LacZ at MOIs of 10 and 30 resulted in approximately 80% and over 90% successful gene transduction, respectively, without morphological changes, cell damage or death (Figure 1). Cardiac fibroblasts also demonstrated high infectivity, although the accurate quantification was difficult.

Effects of Adenoviral HB-EGF Gene Transduction on Cardiomyocytes and Cardiac Fibroblasts *In Vitro*

To explore the direct effects of HB-EGF on cardiomyocytes, we examined cell viability following Ad.HB-EGF infection in two representative injury models of primary cultured cardiomyocytes, Fas-induced apoptosis[34,35] and H_2O_2 oxidative stress injury[34,35] (Figure 2a and b). Both types of stimulus at the predetermined doses efficiently induced cell death in approximately 80% of the cultured cells, and adenoviral HB-EGF gene transduction did not result in significant changes in viability in either of these models at any MOI (Figure 2a and b). However,

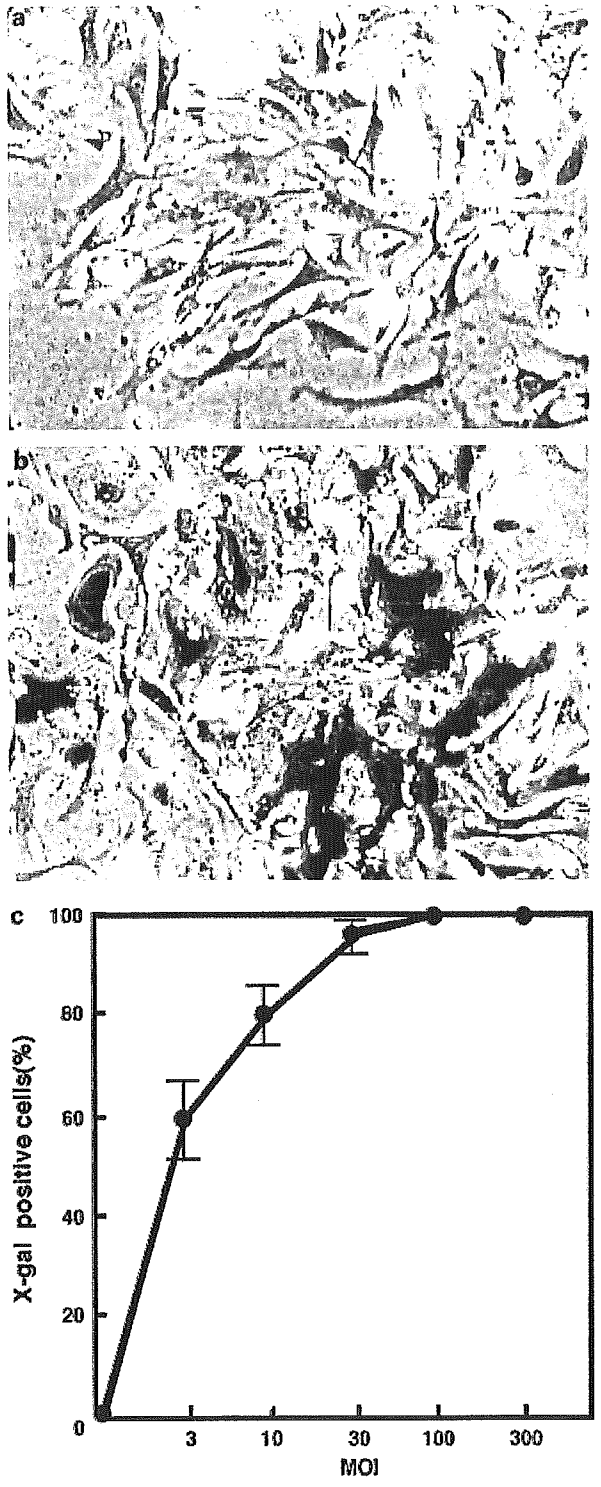

Figure 1 Efficiency of adenoviral gene transduction in primary cultured mouse cardiomyocytes. X-gal staining after Ad.LacZ infection at (**a**) MOI 0 (ie, no infection as a negative control) and (**b**) MOI 10. (**c**) Graph showing adenoviral gene transduction efficiency at various MOIs.

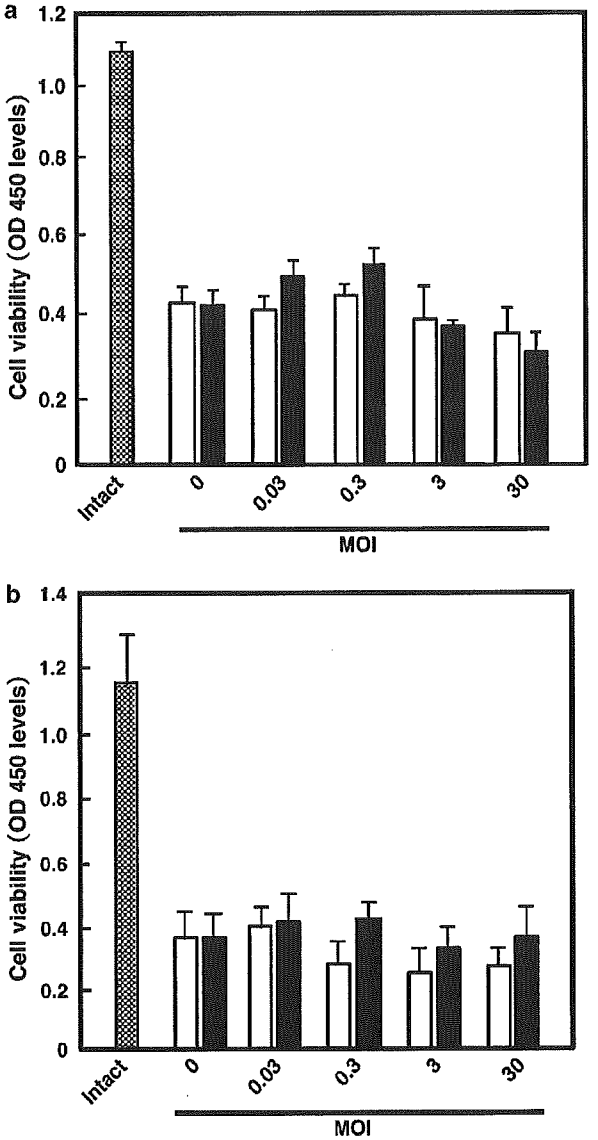

Figure 2 Cell viability after adenoviral HB-EGF gene transduction in two injury models of primary cultured cardiomyocytes. Primary cultured cardiomyocytes were infected with Ad.LacZ (white bar) or Ad.HB-EGF (black bar), and were then exposed to 1 μg/ml anti-Fas antibody and 0.05 μg/ml actinomycin D for 24 h (**a**) or 100 μM H_2O_2 for 1 h (**b**); cell viability was evaluated by WST-8 assay. 'Intact' indicates the control (untreated cells).

cardiomyocytes became significantly enlarged, and their F-actin-containing myofibrils were drastically condensed, enlarged and increased in number following adenoviral HB-EGF gene transduction (Figures 3 and 4).

Next, we explored whether HB-EGF exhibited an inhibitory or stimulatory effect on the growth of cardiac fibroblasts. Both the addition of recombinant HB-EGF and adenoviral HB-EGF gene transduction significantly accelerated the growth of cardiac fibroblasts. (Figure 5). Thus, HB-EGF gene

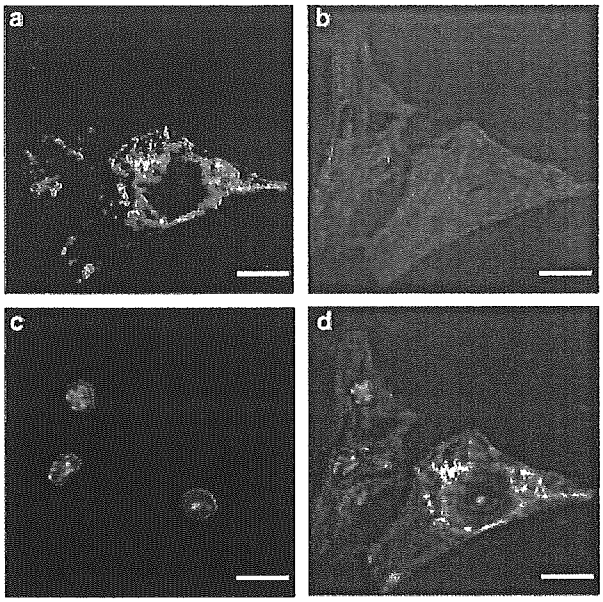

Figure 3 Microscopic images of HB-EGF gene-transduced cardiomyocytes. Confocal microscopic analysis demonstrated apparent hypertrophic changes in individual cardiomyocytes overexpressing HB-EGF after Ad.HB-EGF infection at MOI 30. (**a**) Staining with goat anti-human HB-EGF antibody and Alexa 488-labeled donkey anti-goat secondary antibody, (**b**) staining using rhodamine phalloidin-labeled F-actin, (**c**) staining using Hoechst 33342 (nuclei), and (**d**) merged image. Scale bar = 20 μm.

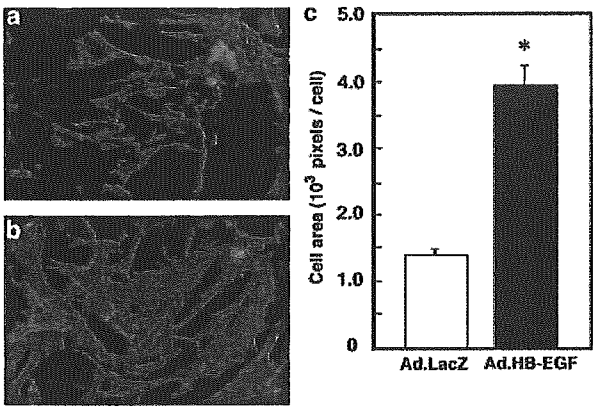

Figure 4 Morphometric and quantitative analysis of HB-EGF gene-transduced cardiomyocytes after Ad.LacZ (**a**) or Ad.HB-EGF (**b**) infection at MOI 30. Hypertrophy as shown by condensation of rhodamine phalloidin-labeled F-actin and enlargement of cell area. Original magnification, × 100. (**c**) Graphic depiction of cell area determined for 500 cardiomyocytes infected with Ad.HB-EGF or Ad.LacZ. *$P<0.001$.

transduction and overexpression conferred a direct hypertrophic effect on cardiomyocytes and a growth-stimulating effect on cardiac fibroblasts, but did not have additive death-inducible or cytoprotective effects on cardiomyocytes.

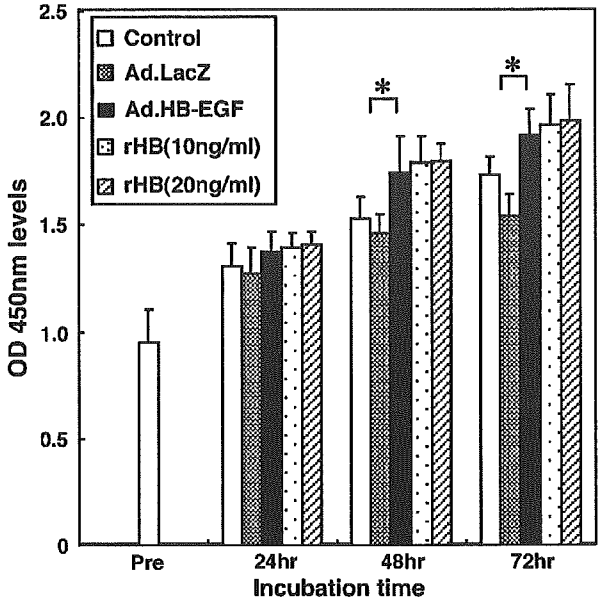

Figure 5 Proliferation of cardiac fibroblasts overexpressing HB-EGF. Cardiac fibroblasts (cell density; 1×10^5/ml) were infected with Ad.LacZ at MOI 30 (shaded bar) or Ad.HB-EGF at MOI 30 (black bar), or were exposed to 10 or 20 ng/ml rHB-EGF for 24, 48, and 72 h; cell proliferation was evaluated by WST-8 assay at OD 450 nm. *$P<0.05$.

Macroscopic Findings after Adenoviral HB-EGF Gene Transduction in the Rabbit MI Model

Recent studies have demonstrated that HB-EGF and EGFR family mRNAs were significantly upregulated around MI lesions,[22,23] and it is for this reason that we injected our adenovirus constructs specifically into this region. X-gal staining after Ad.LacZ injection into this area showed that we were able to drive gene transduction predominantly around the MI (Figure 6a). A number of previous studies have demonstrated retention of transgene expression for at least 3 weeks following *in vivo* adenoviral gene transduction into the heart.[38–40] We have previously described the pathological process in the rabbit MI model in detail, including granulation consisting of myofibroblasts, macrophages and neovasculation at 2 weeks (the subacute stage) and scar formation at 4 weeks (the chronic stage).[37] Together, these results suggested that the period of transgene expression resulting from adenoviral gene transduction would be sufficient for the purposes of this study. In this context, we injected Ad.HB-EGF into the MI injury border area, estimated the risk area and the MI area by TTC and Evans blue dye after 2 weeks (as shown in Figure 6b) and ultraechographically analyzed cardiac function 2 and 4 weeks later. There was no difference in risk area between the two groups (Figure 6c). On the other hand, the ratio of MI area to risk area was seemingly reduced to a small degree by Ad.HB-EGF at 2 weeks post-injection due to hypertrophic changes; however, this reduction was

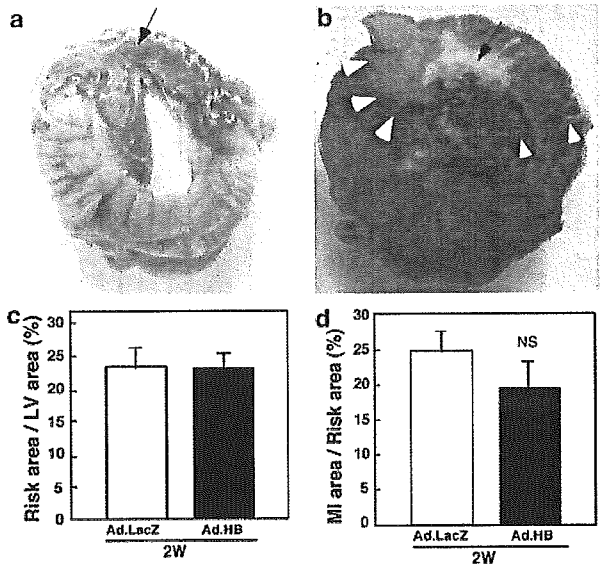

Figure 6 Macroscopic findings after adenoviral HB-EGF gene transduction in a rabbit MI model. (**a**) X-gal staining after Ad.LacZ injection into the border area. The arrow indicates the infarcted area. (**b**) Triphenyl tetrazolium chloride (TTC) and Evans blue staining define the risk areas (arrowheads), MI areas (arrow), and the intact (blue) areas. Graphs showing the risk area (**c**) and the MI area (**d**). Morphometric analysis of TTC/Evans blue-stained macroscopic slides 2 weeks after MI. NS: no significant difference.

not statistically significant (HB-EGF; 19.6±3.5% *vs* LacZ; 24.6±2.9%, $P=0.277$) (Figure 6d).

Cardiac Function and Histological Changes Following Adenoviral HB-EGF Gene Transduction in the Rabbit MI Model

Rabbits that received a control Ad.LacZ injection following MI clearly demonstrated a worsening of cardiac parameters such as left ventricular ejection fraction (LVEF) and left ventricular dimension at end-diastole (LVDd), as assessed by ultraechocardiography (UCG) at 2 and 4 weeks post-MI, compared with sham-operated rabbits that underwent neither adenoviral gene transduction nor MI (Figure 7a and b). Ad.HB-EGF injection after MI neither improved nor further worsened cardiac function, as assessed by LVEF or LVDd at 2 or 4 weeks compared with the Ad.LacZ-treated rabbits. On the other hand, anterior wall thickness (AWt) at 2 weeks (HB-EGF, 2.7±0.3 mm *vs* LacZ, 1.9±0.1 mm, $P<0.05$, Figure 7c) and the ratio of LV weight to body weight at 2 and 4 weeks were significantly increased by Ad.HB-EGF injection (2 weeks: HB-EGF, 1.59±0.06 *vs* LacZ, 1.44±0.03, $P<0.05$; 4 weeks: HB-EGF, 1.67±0.09 *vs* LacZ, 1.40±0.05, $P<0.05$) (Figure 7d); these findings were consistent with macroscopically observed hypertrophic changes (Figure 8). In addition, fibrosis in and around the MI area, which was induced by the MI itself, was increased by injection with Ad.HB-EGF at 2 and 4 weeks post-MI (2 weeks: HB-EGF, 7149±675 pixels *vs* LacZ, 4230±331 pixels, $P<0.001$; 4 weeks: HB-EGF, 6575±534 pixels *vs* LacZ, 4414±494 pixels, $P<0.05$) (Figure 8f).

Accordingly, histological examination revealed that individual cardiomyocytes at the border area were remarkably hypertrophic 2 and 4 weeks after Ad.HB-EGF injections (2 weeks: HB-EGF, 18.76±0.29 μm *vs* LacZ, 16.53±0.34 μm; $P<0.05$; 4 weeks: HB-EGF, 20.49±0.28 μm *vs* LacZ, 18.23±0.40 μm, $P<0.05$) (Figures 9 and 10). Thus, overexpression of HB-EGF markedly induces cardiomyocyte hypertrophy and fibrosis without affecting cardiac function, suggesting that this molecule plays an important role in accelerating the remodeling process after MI.

Characteristic Histological Findings in the MI Area

To clarify the mechanisms responsible for the enhancement of post-MI remodeling in the hearts treated with the HB-EGF gene during the subacute and chronic stages of MI, we performed histological examinations of rabbit hearts at 2 and 4 weeks post-MI. Increases in the number of cells in the MI area 2 and 4 weeks after MI were more prominent in rabbits receiving Ad.HB-EGF than in those receiving control Ad.LacZ (2 weeks: HB-EGF, 235±4 cells/field *vs* LacZ, 145±4 cells/field, $P<0.001$; 4 weeks: HB-EGF, 180±6 cells/field *vs* LacZ, 97±3 cells/field, $P<0.001$) (Figure 11a–c). Likewise, the number of proliferating (Ki-67 positive) cells increased more in the Ad.HB-EGF-treated rabbits than in those treated with Ad.LacZ (2 weeks: HB-EGF, 27.6±1.0 cells/field *vs* LacZ, 7.6±0.3 cells/field, $P<0.001$; 4 weeks: HB-EGF, 25.3±1.4 cells/field *vs* LacZ, 15.8±1.3 cells/field, $P<0.001$) (Figure 11d–f). Immunohistochemical studies demonstrated that these accumulated cells were primarily SMA-positive spindle myofibroblasts at both 2 and 4 weeks (2 weeks: HB-EGF, 62.7±0.8 cells/field *vs* LacZ, 38.0±0.9 cells/field, $P<0.001$; 4 weeks: HB-EGF, 48.6±1.7 cells/field *vs* LacZ, 22.7±1.1 cells/field, $P<0.001$) (Figure 11g–i), and RAM 11-positive macrophages at 2 weeks only (HB-EGF, 18.4±1.0 cells/field *vs* LacZ, 4.2±0.3 cells/field, $P<0.001$) (Figure 11j–l). On the other hand, the finding that more CD31-positive vascular endothelial cells were observed in the border area than in the remote area in both groups suggests an angiogenic effect induced by certain endogenous factors following MI (Figure 11m–o).

Interestingly, these vascular endothelial cells were not further increased by Ad.HB-EGF injections, in contrast to the significant increases observed in total cells, proliferating cells, myofibroblasts and macrophages, suggesting that HB-EGF most likely lacks angiogenic potential.

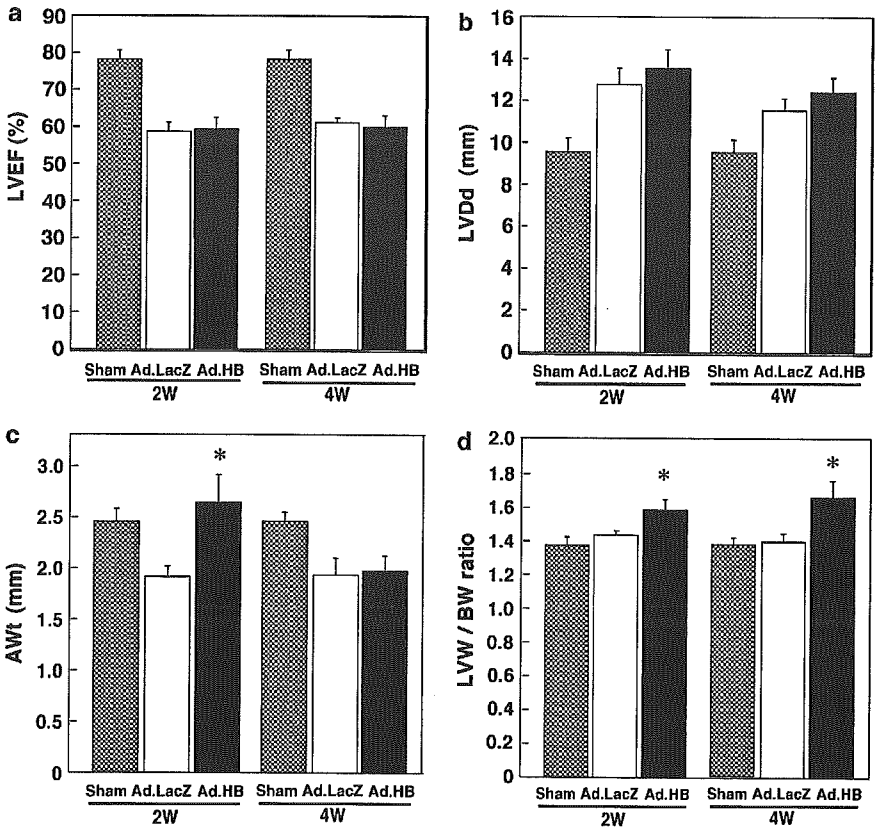

Figure 7 Echocardiographic measurements and left ventricular (LV) weight after adenoviral HB-EGF gene transduction in the postinfarct rabbit heart. Graphs showing the (**a**) LVEF, (**b**) LV size, (**c**) wall thickness, and (**d**) LV weight to body weight at 2 and 4 weeks after Ad.HB-EGF gene transduction in MI rabbits. Cardiac function parameters were assessed by echocardiographic examination. LVEF: left ventricular ejection fraction; LVDd: left ventricular dimension at end-diastole; AWt: anterior wall thickness; LVW: LV weight; BW: indicated body weight. 'Sham' indicates sham-operated rabbits without MI or adenoviral transduction. $^*P<0.05$.

Apoptosis in the MI Area after Adenoviral HB-EGF Gene Transduction

To estimate apoptosis in the MI area, TUNEL staining was performed. Unexpectedly, the number of TUNEL-positive cells was increased by Ad.HB-EGF injection at 2 weeks after MI (HB-EGF, $1.95\pm0.10\%$ *vs* LacZ, $1.04\pm0.09\%$, $P<0.001$) (Figure 12). Notably, most of the TUNEL-positive cells were costained with the anti-RAM11 antibody (Figure 13a and b), but not with anti-SMA antibody (Figure 13c), nor by markers for cardiomyocytes such as troponin I (Figure 13d). Moreover, TUNEL-positive signals were detected in the cytoplasm of some macrophages with intact nuclei. Thus, the TUNEL-positive cells may be not only apoptotic macrophages, but also viable macrophages that had phagocytosed other apoptotic cells (Figure 13b). Thus, *in vivo* HB-EGF gene transduction stimulated the activation of noncardiomyocytes, including macrophages, fibroblasts and myofibroblasts, but not endothelial cells, in and around the MI area, while at the same time inducing cardiac hypertrophy.

Discussion

This is the first study to explore directly the *in vivo* effects of overexpressed HB-EGF on heart remodeling after reperfused MI. In addition, our unique adenoviral gene transduction and overexpression approach allowed a preliminary assessment of the potential utility of HB-EGF in gene therapy. Overexpressed HB-EGF in the MI lesion did not result in a beneficial or therapeutic outcome, in contrast to results observed with HGF or IGF in rodent MI models, but rather exacerbated the remodeling process through the activation of specific types of noncardiomyocytes.

To identify the HB-EGF-related biological mechanism underlying heart failure, distinguishing the various phenotypic effects of HB-EGF from those of HGF and IGF may prove useful, because despite their differences all of these factors are essential cardiogenic growth factors as well as potent inducers of cardiac hypertrophy.[27,29,41] The most important difference between HB-EGF and HGF/IGF, which accounts for the observed discrepancy, is

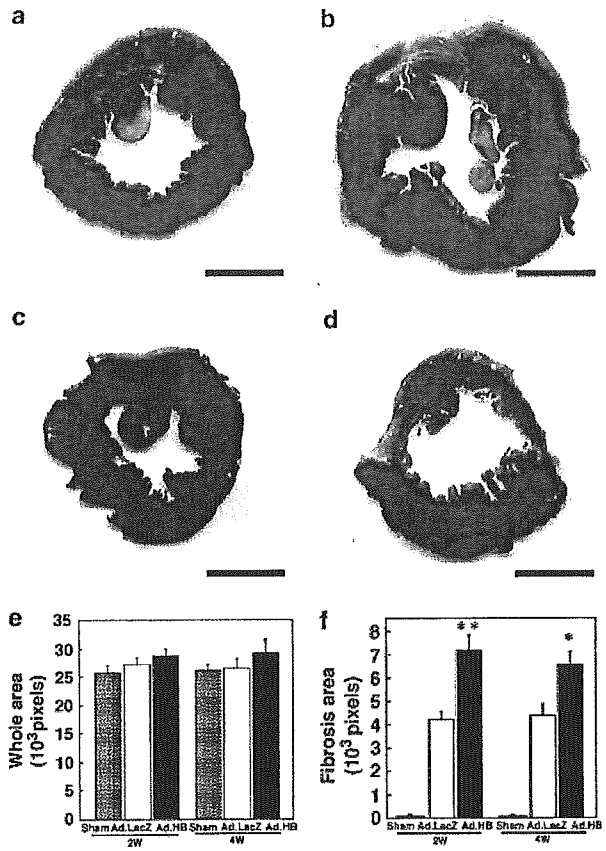

Figure 8 Macroscopic findings and histological analyses of transverse sections of hearts after adenoviral HB-EGF gene transduction. Fibrosis areas were stained blue with Masson's trichrome. (**a**) Ad.LacZ group (control) at 2 weeks after MI, (**b**) Ad.HB-EGF group at 2 weeks after MI, (**c**) Ad.LacZ group at 4 weeks after MI, (**d**) Ad.HB-EGF group at 4 weeks after MI. Graphs showing the whole areas (**e**) and fibrosis areas (**f**). The stained areas were morphometrically analyzed by counting pixels. Scale bar = 5 mm, $*P<0.05$, $**P<0.001$.

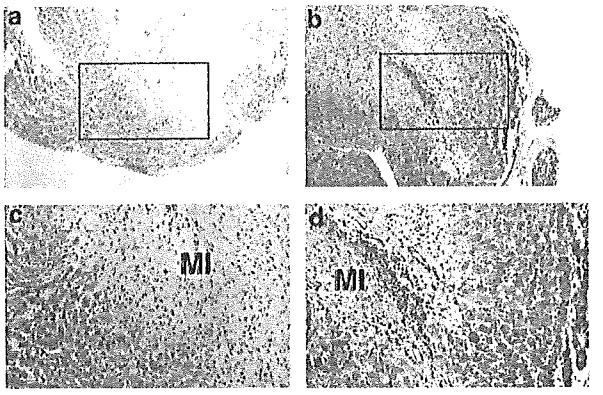

Figure 9 Histological findings at the MI border area after treatment. H–E-stained slides of LV 2 weeks post-MI. (**a**), (**c**) Ad.LacZ-treated rabbits and (**b**), (**d**) Ad.HB-EGF-treated rabbits. Squared-in areas in (**a**) and (**b**) (original magnification ×100) were magnified in (**c**) and (**d**) (original magnification ×400), respectively.

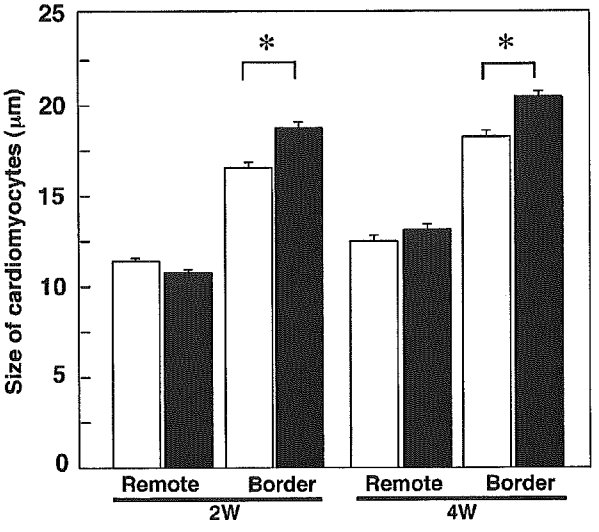

Figure 10 Size of cardiomyocytes at the remote and border areas of MI after treatment. The size of individual cardiomyocytes at the remote and border areas was morphometrically analyzed. $*P<0.001$.

the lack of a direct cytoprotective effect of HB-EGF on cardiomyocytes, in contrast to the potent cytoprotective effect observed for HGF and IGF in injured hearts.[27,29,41] This is a unique feature of HB-EGF, because most organogenic and/or organotrophic growth factors exert direct antiapoptotic effects, for example, HGF or IGF in mouse or rat cardiomyocytes[26–29] and HB-EGF in the small intestine.[42] In this regard, future studies to explore the differences among the molecules and signal transduction pathways involved in the activity of each growth factor would be biologically important.

Another important feature that differentiated HB-EGF from HGF and IGF was its observed lack of angiogenic activity. It should be noted that improvement of cardiac dysfunction after MI has been successfully achieved by gene therapy using angiogenic factors that do not directly act on cardiomyocytes.[29,43] This fact suggests that angiogenesis plays a crucial role in postinfarction remodeling, and that the absence of an angiogenic effect of overexpressed HB-EGF may be largely responsible for its lack of therapeutic action.

In addition, HB-EGF was revealed to have a mitogenic effect on fibroblasts, in contrast to the potent antifibrotic effect of HGF following MI.[27] Moreover, the characteristic finding after HB-EGF gene transduction was prominent accumulation of SMA-positive myofibroblasts and macrophages in the MI-affected areas. We previously reported that the infiltrating cells at the subacute stage post-MI

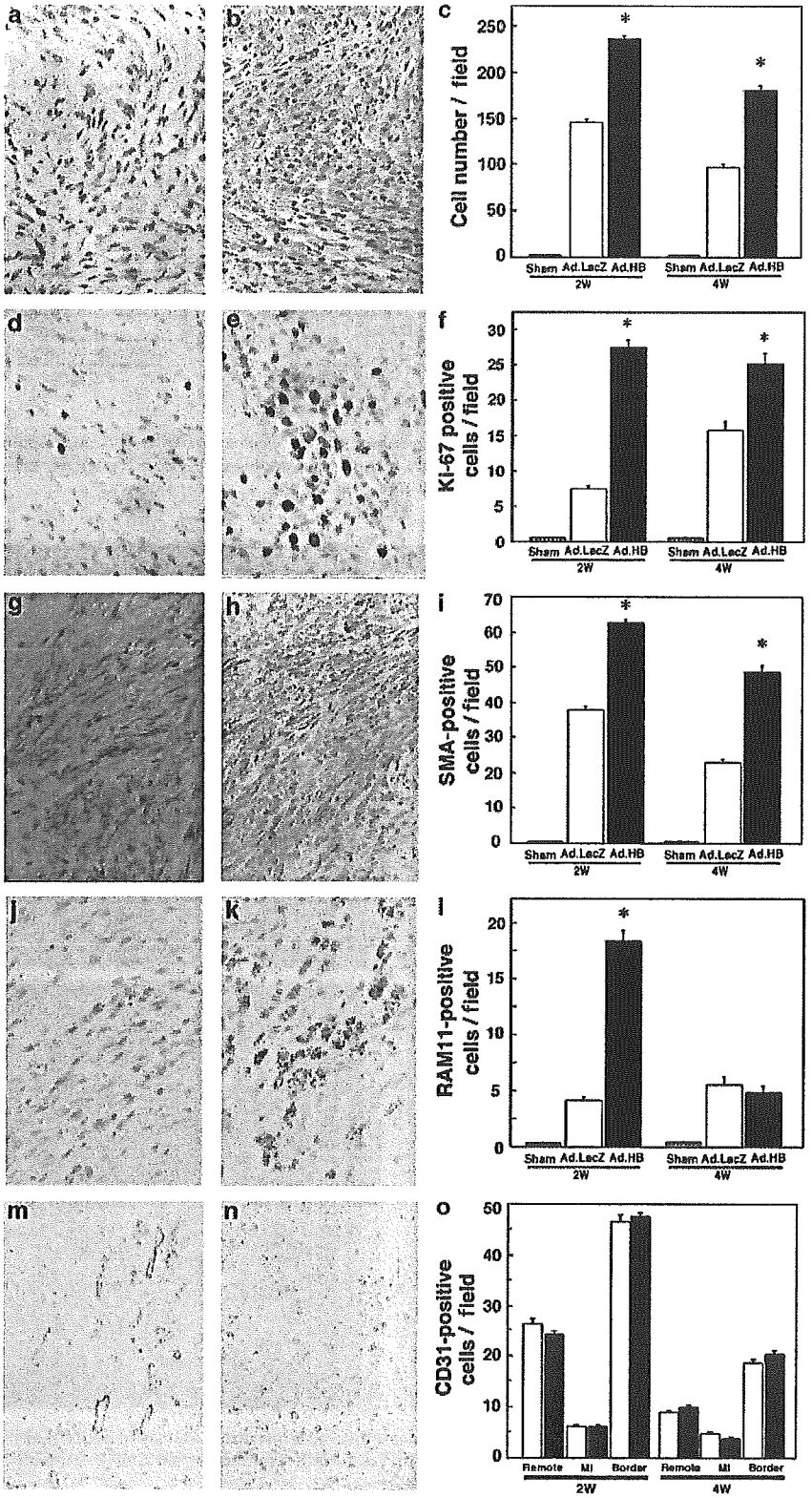

Figure 11 Histological and immunohistochemical findings in the MI area post-treatment. (**a**, **b**) H–E-stained-tissues, and immunohistochemically stained-tissues using (**d**, **e**) anti-Ki-67, (**g**, **h**) anti-SMA, (**j**, **k**) anti-RAM11, or (**m**, **n**) anti-CD31 antibodies 2 weeks after MI are shown (original magnification, × 400 for **a**, **b**, **d**, **e**, **g**, **h**, **j** and **k**, and × 100 for **m** and **n**). The number of positive cells in the field 2 and 4 weeks after MI were calculated and shown in the graphs (**c**, **f**, **i**, **l**, and **o**). *$P<0.001$.

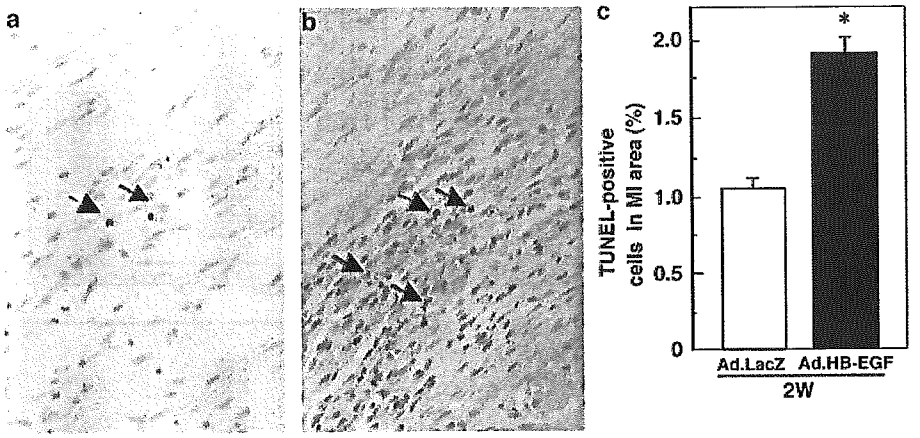

Figure 12 TUNEL staining in the MI area. TUNEL-positive cells (arrows) in the MI area 2 weeks after each treatment are shown. (**a**) and (**b**) indicate Ad.LacZ- and Ad.HB-EGF-treated rabbits, respectively. (**c**) The percentage of TUNEL-positive cells in the MI area was calculated by morphometric and quantitative analyses . $^*P<0.001$.

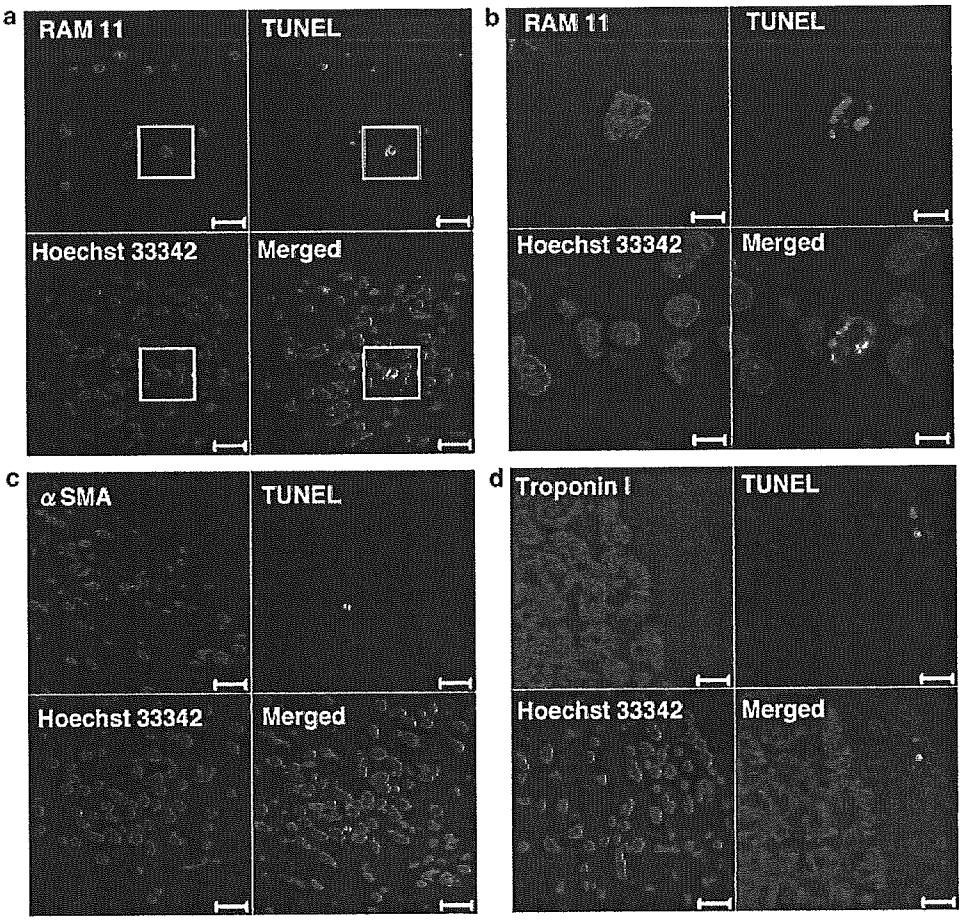

Figure 13 Immunofluorescent-TUNEL staining in the MI area. Laser confocal-microscopic analysis of slides that were triple-stained with TUNEL and (**a**, **b**) anti-RAM11, (**c**) anti-SMA and (**d**) anti-troponin I antibodies, and Hoechst 33342. Squared areas within (**a**) were magnified and shown in (**b**). Scale bars, 20 μm (**a**, **c**, **d**) and 5 μm (**b**).

were primarily macrophages, endothelial cells, and myofibroblasts, and that all of these cell types were entering apoptosis at an elevated rate.[37] Thus, the previously unknown factor that activates fibroblasts, myofibroblasts, and macrophages during post infarction remodeling is now strongly suggested to be

HB-EGF. Taken together with the lack of an agonistic death-inducible effect of HB-EGF directly on cardiomyocytes, pathologically upregulated HB-EGF may be responsible for activating these specific types of noncardiomyocytes, thus exacerbating post-MI remodeling.

The detailed molecular mechanisms by which HB-EGF activates these specific types of noncardiomyocytes remain to be elucidated. It was previously reported that HB-EGF stimulated the mitogenic and motogenic activities of smooth muscle cells,[4,7] and also that it reduced the expression of SMA in fibroblasts.[17] HB-EGF may play a regulatory role in the growth of fibroblasts and their transformation to myofibroblasts in the heart, as was suggested for the postinfarct kidney.[17] However, the biological relationship between HB-EGF and macrophages has yet to be studied, so future work to explore these molecular mechanisms would be interesting and fruitful. In this study, the overexpressed HB-EGF may consist not only of soluble HB-EGF, a potent mitogen for diverse cell types, but also membrane-bound proHB-EGF, whose functions may be diverse depending on cell types. In this context, future biological studies comparing the physiological and pathological effects of proHB-EGF on the heart with those of soluble HB-EGF may be of interest, although a suitable experimental system should be carefully established.

Finally, the recent finding that shedding of proHB-EGF resulted in cardiac hypertrophy suggests that upregulated HB-EGF might play a central role in hypertensive heart diseases.[24,25] However, overexpression of HGF and IGF induced cardiac hypertrophy, but inconsistently exhibited potent therapeutic and beneficial effects on the injured heart, including that damaged by MI.[27–29] Taken together with these facts, HB-EGF-induced cardiac hypertrophy may not be a sole or direct source of pathogenesis in MI, even though cardiac hypertrophy may, in fact, be involved in specific types of heart failure. In this context, the present results importantly imply that HB-EGF-induced exacerbation of remodeling may be a novel pathological mechanism for MI.

In conclusion, upregulated HB-EGF plays a pathological role in MI by activating specific types of noncardiomyocytes, leading to exacerbation of remodeling after MI. This novel fact may be useful for developing new therapeutics as well as for elucidating the mechanism of different types of heart failure, including MI.

Acknowledgements

This study was supported in part by Suzuken Memorial Foundation and a Grant-in-Aid for Scientific Research (C) from the Ministry of Education, Culture, Sports, Science and Technology of Japan. We thank Hatsue Oshika and Akiko Tsujimoto for their technical assistance.

References

1 Higashiyama S, Abraham JA, Miller J, *et al.* A heparin-binding growth factor secreted by macrophage-like cells that is related to EGF. Science 1991;251: 936–939.
2 Prenzel N, Zwick E, Daub H, *et al.* EGF receptor transactivation by G-protein-coupled receptors requires metalloproteinase cleavage of proHB-EGF. Nature 1999;402:884–888.
3 Ito N, Kawata S, Tamura S, *et al.* Heparin-binding EGF-like growth factor is a potent mitogen for rat hepatocytes. Biochem Biophys Res Commun 1994;198:25–31.
4 Higashiyama S, Abraham JA, Klagsbrun M. Heparin-binding EGF-like growth factor stimulation of smooth muscle cell migration: dependence on interactions with cell surface heparan sulfate. J Cell Biol 1993;122: 933–940.
5 Kiso S, Kawata S, Tamura S, *et al.* Liver regeneration in heparin-binding EGF-like growth factor transgenic mice after partial hepatectomy. Gastroenterology 2003; 124:701–707.
6 Iwamoto R, Mekada E. Heparin-binding EGF-like growth factor: a juxtacrine growth factor. Cytokine Growth Factor Rev 2000;11:335–344.
7 Miyagawa J, Higashiyama S, Kawata S, *et al.* Localization of heparin-binding EGF-like growth factor in the smooth muscle cells and macrophages of human atherosclerotic plaques. J Clin Invest 1995;95: 404–411.
8 Kalmes A, Daum G, Clowes AW. EGFR transactivation in the regulation of SMC function. Ann NY Acad Sci 2001;947:42–54; discussion 54–45.
9 Lemjabbar H, Basbaum C. Platelet-activating factor receptor and ADAM10 mediate responses to *Staphylococcus aureus* in epithelial cells. Nat Med 2002;8: 41–46.
10 Fu S, Bottoli I, Goller M, *et al.* Heparin-binding epidermal growth factor-like growth factor, a v-Jun target gene, induces oncogenic transformation. Proc Natl Acad Sci USA 1999;96:5716–5721.
11 Marikovsky M, Breuing K, Liu PY, *et al.* Appearance of heparin-binding EGF-like growth factor in wound fluid as a response to injury. Proc Natl Acad Sci USA 1993;90:3889–3893.
12 Tokumaru S, Higashiyama S, Endo T, *et al.* Ectodomain shedding of epidermal growth factor receptor ligands is required for keratinocyte migration in cutaneous wound healing. J Cell Biol 2000;151:209–220.
13 Nguyen HT, Bride SH, Badawy AB, *et al.* Heparin-binding EGF-like growth factor is up-regulated in the obstructed kidney in a cell- and region-specific manner and acts to inhibit apoptosis. Am J Pathol 2000;156:889–898.
14 Sakai M, Zhang M, Homma T, *et al.* Production of heparin binding epidermal growth factor-like growth factor in the early phase of regeneration after acute renal injury. Isolation and localization of bioactive molecules. J Clin Invest 1997;99:2128–2138.
15 Xia G, Rachfal AW, Martin AE, *et al.* Upregulation of endogenous heparin-binding EGF-like growth factor (HB-EGF) expression after intestinal ischemia/reperfusion injury. J Invest Surg 2003;16:57–63.
16 Pillai SB, Hinman CE, Luquette MH, *et al.* Heparin-binding epidermal growth factor-like growth factor protects rat intestine from ischemia/reperfusion injury. J Surg Res 1999;87:225–231.

17 Kirkland G, Paizis K, Wu LL, *et al.* Heparin-binding EGF-like growth factor mRNA is upregulated in the peri-infarct region of the remnant kidney model: *in vitro* evidence suggests a regulatory role in myofibroblast transformation. J Am Soc Nephrol 1998;9: 1464–1473.
18 Iwamoto R, Yamazaki S, Asakura M, *et al.* Heparin-binding EGF-like growth factor and ErbB signaling is essential for heart function. Proc Natl Acad Sci USA 2003;100:3221–3226.
19 Jackson LF, Qiu TH, Sunnarborg SW, *et al.* Defective valvulogenesis in HB-EGF and TACE-null mice is associated with aberrant BMP signaling. EMBO J 2003; 22:2704–2716.
20 Nakamura Y, Handa K, Iwamoto R, *et al.* Immunohistochemical distribution of CD9, heparin binding epidermal growth factor-like growth factor, and integrin alpha3beta1 in normal human tissues. J Histochem Cytochem 2001;49:439–444.
21 Fujino T, Hasebe N, Fujita M, *et al.* Enhanced expression of heparin-binding EGF-like growth factor and its receptor in hypertrophied left ventricle of spontaneously hypertensive rats. Cardiovasc Res 1998; 38:365–374.
22 Iwabu A, Murakami T, Kusachi S, *et al.* Concomitant expression of heparin-binding epidermal growth factor-like growth factor mRNA and basic fibroblast growth factor mRNA in myocardial infarction in rats. Basic Res Cardiol 2002;97:214–222.
23 Tanaka N, Masamura K, Yoshida M, *et al.* A role of heparin-binding epidermal growth factor-like growth factor in cardiac remodeling after myocardial infarction. Biochem Biophys Res Commun 2002;297: 375–381.
24 Asakura M, Kitakaze M, Takashima S, *et al.* Cardiac hypertrophy is inhibited by antagonism of ADAM12 processing of HB-EGF: metalloproteinase inhibitors as a new therapy. Nat Med 2002;8:35–40.
25 Shah BH, Catt KJ. A central role of EGF receptor transactivation in angiotensin II-induced cardiac hypertrophy. Trends Pharmacol Sci 2003;24:239–244.
26 Taniyama Y, Morishita R, Aoki M, *et al.* Angiogenesis and antifibrotic action by hepatocyte growth factor in cardiomyopathy. Hypertension 2002;40:47–53.
27 Li Y, Takemura G, Kosai K, *et al.* Postinfarction treatment with an adenoviral vector expressing hepatocyte growth factor relieves chronic left ventricular remodeling and dysfunction in mice. Circulation 2003; 107:2499–2506.
28 Li Q, Li B, Wang X, *et al.* Overexpression of insulin-like growth factor-1 in mice protects from myocyte death after infarction, attenuating ventricular dilation, wall stress, and cardiac hypertrophy. J Clin Invest 1997;100:1991–1999.
29 Su EJ, Cioffi CL, Stefansson S, *et al.* Gene therapy vector-mediated expression of insulin-like growth factors protects cardiomyocytes from apoptosis and enhances neovascularization. Am J Physiol Heart Circ Physiol 2003;284:H1429–H1440.
30 Chen SH, Chen XH, Wang Y, *et al.* Combination gene therapy for liver metastasis of colon carcinoma *in vivo*. Proc Natl Acad Sci USA 1995;92:2577–2581.
31 Terazaki Y, Yano S, Yuge K, *et al.* An optimal therapeutic expression level is crucial for suicide gene therapy for hepatic metastatic cancer in mice. Hepatology 2003;37:155–163.
32 Aoyama T, Takemura G, Maruyama R, *et al.* Molecular mechanisms of non-apoptosis by Fas stimulation alone versus apoptosis with an additional actinomycin D in cultured cardiomyocytes. Cardiovasc Res 2002;55: 787–798.
33 Ogasawara J, Watanabe-Fukunaga R, Adachi M, *et al.* Lethal effect of the anti-Fas antibody in mice. Nature 1993;364:806–809.
34 Takemura G, Kato S, Aoyama T, *et al.* Characterization of ultrastructure and its relation with DNA fragmentation in Fas-induced apoptosis of cultured cardiac myocytes. J Pathol 2001;193:546–556.
35 Toraason M, Wey H, Woolery M, *et al.* Arachidonic acid supplementation enhances hydrogen peroxide induced oxidative injury of neonatal rat cardiac myocytes. Cardiovasc Res 1995;29:624–628.
36 Villarreal FJ, Kim NN, Ungab GD, *et al.* Identification of functional angiotensin II receptors on rat cardiac fibroblasts. Circulation 1993;88:2849–2861.
37 Takemura G, Ohno M, Hayakawa Y, *et al.* Role of apoptosis in the disappearance of infiltrated, proliferated interstitial cells after myocardial infarction. Circ Res 1998;82:1130–1138.
38 Leor J, Quinones MJ, Patterson M, *et al.* Adenovirus-mediated gene transfer into infarcted myocardium: feasibility, timing, and location of expression. J Mol Cell Cardiol 1996;28:2057–2067.
39 Barr E, Carroll J, Kalynych AM, *et al.* Efficient catheter-mediated gene transfer into the heart using replication-defective adenovirus. Gene Therapy 1994;1:51–58.
40 Chu D, Sullivan CC, Weitzman MD, *et al.* Direct comparison of efficiency and stability of gene transfer into the mammalian heart using adeno-associated virus versus adenovirus vectors. J Thorac Cardiovasc Surg 2003;126:671–679.
41 Huang CY, Hao LY, Buetow DE. Insulin-like growth factor-induced hypertrophy of cultured adult rat cardiomyocytes is L-type calcium-channel-dependent. Mol Cell Biochem 2002;231:51–59.
42 Michalsky MP, Kuhn A, Mehta V, *et al.* Heparin-binding EGF-like growth factor decreases apoptosis in intestinal epithelial cells *in vitro*. J Pediatr Surg 2001;36:1130–1135.
43 Siddiqui AJ, Blomberg P, Wardell E, *et al.* Combination of angiopoietin-1 and vascular endothelial growth factor gene therapy enhances arteriogenesis in the ischemic myocardium. Biochem Biophys Res Commun 2003;310:1002–1009.

Research Article

Survivin-Responsive Conditionally Replicating Adenovirus Exhibits Cancer-Specific and Efficient Viral Replication

Junichi Kamizono,[1,3] Satoshi Nagano,[1,2,3] Yoshiteru Murofushi,[1] Setsuro Komiya,[3] Hisayoshi Fujiwara,[4] Toyojiro Matsuishi,[1,2] and Ken-ichiro Kosai[1,2]

[1]Division of Gene Therapy and Regenerative Medicine, Cognitive and Molecular Research Institute of Brain Diseases and [2]Department of Pediatrics and Child Health, Kurume University, Kurume, Japan; [3]Department of Orthopaedic Surgery, Graduate School of Medical and Dental Sciences, Kagoshima University, Kagoshima, Japan; and [4]Department of Cardiology, Respiratory and Nephrology, Regeneration and Advanced Medical Science, Graduate School of Medicine, Gifu University, Gifu, Japan

Abstract

Although a conditionally replicating adenovirus (CRA) exhibiting cancer-selective replication and induction of cell death is an innovative potential anticancer agent, current imperfections in cancer specificity and efficient viral replication limit the usefulness of this technique. Here, we constructed *survivin*-responsive CRAs (Surv.CRAs), in which expression of the wild-type or mutant adenoviral early region 1A (*E1A*) gene is regulated by the promoter of *survivin*, a new member of the inhibitor of apoptosis gene family. We explored the cancer specificity and effectiveness of viral replication of Surv.CRAs, evaluating their potential as a treatment for cancer. The *survivin* promoter was strongly activated in all cancers examined at levels similar to or even higher than those seen for representative strong promoters; in contrast, low activity was observed in normal cells. Surv.CRAs efficiently replicated and potently induced cell death in most types of cancer. In contrast, minimal viral replication in normal cells did not induce any detectable cytotoxicity. A single injection of Surv.CRAs into a preestablished tumor expressing *survivin*, even at relatively low levels, induced significant tumor death and inhibition of tumor growth. Furthermore, Surv.CRAs were superior to telomerase-dependent CRAs, one of the most effective CRAs that have been examined to date, both in terms of cancer specificity and efficiency. Thus, Surv.CRAs are an attractive potential anticancer agent that could effectively and specifically treat a variety of cancers. (Cancer Res 2005; 65(12): 5284-91)

Introduction

Conditionally replicating adenoviruses (CRAs), which selectively replicate in and kill tumor cells, may be an attractive tool for innovative cancer therapy (1). Achievement of both cancer specificity and efficient viral replication is critical for any CRA-oriented strategy. The CRAs that have been reported to date can primarily be classified into one of two groups (1). The first category employs the strategy of attenuating viral replication in normal cells by mutating cell cycle–inducing adenoviral genes necessary for viral replication; representatives of this group are the mutant type (MT) adenoviruses lacking an RB-binding site within early region 1A (E1A) and the MT adenoviruses lacking a p53-binding protein encoded by the early region 1B (*E1B*)-55K gene (2–4). Although these CRAs exhibit potential in cancer cells, these viruses do replicate and cause some cytopathic effects in normal cells (4–6). The second group of CRAs alters the regulation of E1A expression. *E1A* is the first gene to be transcribed after infection with wild-type (WT) adenoviruses, transactivating the viral and cellular genes critical for producing infective adenoviruses. CRAs of this category reproduce in a tumor-specific manner by replacing the native E1A promoter with a tissue- and tumor-specific promoter, such as the prostate-specific antigen promoter (7), the α-fetoprotein promoter (8), the midkine promoter (9), or the tyrosinase promoter (10). Although previous studies of this CRA strategy have been promising, the use of tissue-specific promoters has the disadvantage of targeting only limited types of cancer. In addition, these promoters show insufficient cancer specificity (leaky transactivation in normal cells) and weak activity even in cancer cells. Thus, viral targeting and replication for previously reported CRAs may not have achieved sufficient efficiency or cancer specificity. The use of a novel and ideal promoter able to induce strong expression in a cancer-specific manner is crucial to circumventing these problems.

Survivin, a new member of the inhibitor of apoptosis gene family, was reported to be expressed in high levels in cancerous but not normal tissues (11). Clinical studies have indicated a positive correlation between high *survivin* expression levels and a poor prognosis, an accelerated rate of recurrence, and an increased resistance to therapy in cancer patients (12). *Survivin* is predominantly expressed during the G_2-M phase of the cell cycle, functioning in mitosis via interactions with microtubules (13). In addition, the *survivin* promoter successfully regulates transgene expression in a cancer-specific manner (14). Moreover, studies have suggested that a putative region of the *survivin* promoter is likely responsible for the induction of cancer-specific expression in tumors at high levels (15, 16). The promoter contains multiple cell cycle–dependent elements and a cell cycle gene homology region, which may control expression of various G_2-M-regulated genes, including the *survivin* gene, in a manner correlating with G_2-M cell cycle periodicity (13, 15–17).

In this study, we generated and analyzed two *survivin*-responsive CRAs (Surv.CRAs). Surv.CRAwt and Surv.CRAmt expressed WT and MT E1A under the control of the *survivin* promoter, respectively. We finally compared these Surv.CRAs to a recently reported CRA, in which E1A is regulated by the telomerase reverse transcriptase (TERT) promoter (Tert.CRA), currently one of the best CRAs available (18–20).

Materials and Methods

Cell lines. The human cell lines MKN-1 and MKN-45 (gastric cancer cell lines); HCT-15, LoVo, and Colo-205 (colon cancer cell lines); HepG2 and

Note: J. Kamizono and S. Nagano contributed equally to this work.

Requests for reprints: Ken-ichiro Kosai, Division of Gene Therapy and Regenerative Medicine, Cognitive and Molecular Research Institute of Brain Diseases, Kurume University, 67 Asahi-machi, Kurume, 830-0011, Japan. Phone: 81-942-31-7910; Fax: 81-942-31-7911; E-mail: kosai@med.kurume-u.ac.jp.

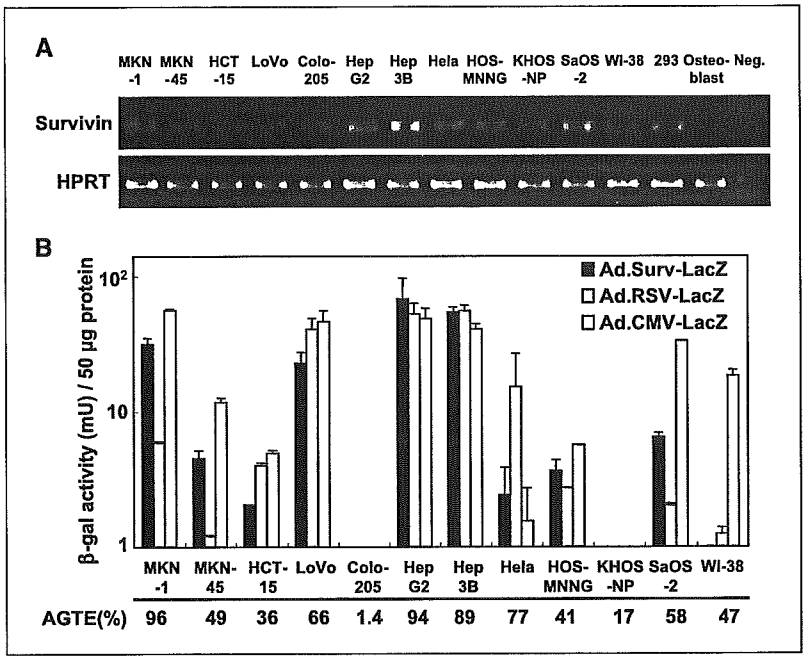

Figure 1. *Survivin* mRNA expression (*A*) and promoter activity (*B*). *A*, endogenous *survivin* mRNA was detected by PCR. The *HPRT* gene was amplified as an internal control. *Neg*, template was omitted from the reaction as a negative control. *B*, β-gal enzyme activity was detected 48 hours after infection with Ad.Surv-LacZ, Ad.CMV-LacZ, or Ad.RSV-LacZ at an MOI of 30. *Columns*, mean of three independent experiments; *bars*, ±SE. AGTE is presented as the percentage of X-gal-stained cells observed among the total cells at 48 hours after Ad.CMV-LacZ infection at an MOI of 30.

Hep3B (hepatoma cell lines); HeLa (a cervical cancer cell line); SaOS-2, HOS-MNNG, and KHOS-NP (osteosarcoma cell lines); and WI-38 (a primary lung fibroblast) were maintained in DMEM supplemented with penicillin/streptomycin and 10% fetal bovine serum. Primary human osteoblasts, obtained from Bio Whittaker (Walkersville, MD), were maintained according to the manufacturer's protocol.

Generation of adenoviruses. A region of the mouse *survivin* gene promoter (−173 to −19), which contains two cell cycle–dependent elements and one cell cycle gene homology region, was obtained from mouse genomic DNA by PCR using the following primers: sense (S)-Surv.pr 5′-AGATGGGCGTGGGGCGGGAC-3′ and antisense (AS)-Surv.pr 5′-TCCGCCAAGACGACTCAAAC-3′. Generation of Surv.CRAwt, Surv.CRAmt, and Tert.CRAwt viruses, which contained WT or MT E1A downstream of either the *survivin* or TERT promoter (−181 to +79; kindly provided by Dr. S. Kyo, Kanazawa University School of Medicine; ref. 21), E1BΔ55K downstream of the cytomegalovirus immediate-early gene enhancer/promoter (CMV promoter), and the enhanced green fluorescent protein (*EGFP*) gene downstream of the CMV promoter, was done using a novel method developed by our group (22).

An E1-deleted replication-defective adenovirus expressing EGFP (Ad.ΔE1) and E1-deleted adenoviruses expressing the *LacZ* gene under the control of the Rous sarcoma virus long-terminal repeat (RSV promoter), the CMV promoter, the *survivin* promoter, or the TERT promoter (Ad.RSV-LacZ, Ad.CMV-LacZ, Ad.Surv-LacZ, and Ad.Tert-LacZ, respectively) were generated and prepared as described previously (23).

Reverse transcription-PCR analysis. Extraction of total RNA from the cells and the semiquantitative reverse transcription-PCR (RT-PCR) analyses were done as described previously (24), with the following primer sets and annealing temperatures: S-Surv 5′-CCCTTGGTGAATTTTTGAAA-3′ and AS-Surv 5′-TGGTGCCACTTTCAAGACAA-3′ for human *survivin* at 56°C; S-TERT 5′-TTCCTGCACTGGCTGATGAGTGT-3′ and AS-TERT 5′-CGC-TCGGCCCTCTTTTCTCTG-3′ for human *TERT* at 59°C (25); and S-HPRT 5′-CCTGCTGGATTACATTAAAGCACTG-3′ and AS-HPRT 5′-AAGGGCATA-TCCAACAACAA-3′ for hypoxanthine guanine phosphoribosyl transferase (*HPRT*) as an internal control at 57°C (24, 26).

Promoter activities and adenoviral gene transduction efficiency. Cells (5×10^5 cells per plate) were infected with Ad.CMV-LacZ, Ad.RSV-LacZ, Ad.Surv-LacZ, or Ad.Tert-LacZ at a multiplicity of infection (MOI) of 30 for 24 hours. After harvesting, cellular β-galactosidase (β-gal) activity was measured as previously described (27).

The adenoviral gene transduction efficiency (AGTE) for each cell *in vitro* was determined 48 hours after infection with Ad.CMV-LacZ at an MOI of 30, as previously described (27–29).

Flow cytometric analysis. After infection with each adenovirus, cells were detached with trypsin and fixed in 4% paraformaldehyde. The percentage of EGFP-positive cells was then analyzed by flow cytometry on a FACSCalibur using CELLQuest software (Becton Dickinson, San Jose, CA).

Cytotoxic effects *in vitro*. After plating in 96-well plates, cells were infected with each adenovirus at a variety of MOIs. Cell viability was determined 3 and 5 days after adenoviral infection using a WST-8 assay (Dojindo Laboratories, Mashiki, Japan) according to the manufacturer's protocol.

Therapeutic effects *in vivo* in animal experiments. HOS-MNNG cells (5×10^6 cells) were injected s.c. into the back of 5-week-old male BALB/c athymic nude mice. After the s.c. tumors reached 6 to 10 mm in diameter, the mice were randomly divided into three groups. Each group was given a single injection of 1×10^8 plaque-forming unit (pfu) Surv.CRAwt ($n = 9$), Surv.CRAmt ($n = 8$), or Ad.ΔE1 ($n = 8$) in 50 μL of 10 mmol/L Tris-HCl (pH 7.4)/1 mmol/L $MgCl_2$/10% (v/v) glycerol/hexadimethrine bromide (20 μg/mL) into the s.c. tumor. In another comparative experiment, tumor-bearing mice were infected with Tert.CRAwt ($n = 9$), Surv.CRAwt ($n = 8$), or Ad.ΔE1 ($n = 11$) as described above. Tumor size was then monitored twice a week using digital calipers. Tumor volume was calculated according to the following formula: volume = long axis × (short axis)^2 × 0.5 (29, 30).

For histopathologic analysis, the tumors were fixed in 10% buffered formalin, embedded in paraffin, cut into 4-μm serial sections, and stained with H&E.

The protocol for this animal experiment was approved by the Animal Research Committee of Kurume University. All animal experiments were done in accordance with the NIH Guidelines for the Care and Use of Laboratory Animals.

Statistical analysis. Data are represented as the means ± SE. Statistical significance was determined using the Student's t test. $P < 0.05$ were considered to indicate statistical significance.

Results

***Survivin* mRNA was expressed in various cancer cell lines.** The RT-PCR analyses showed that *survivin* mRNA was expressed in multiple cancer cells derived from a variety of tissue origins;

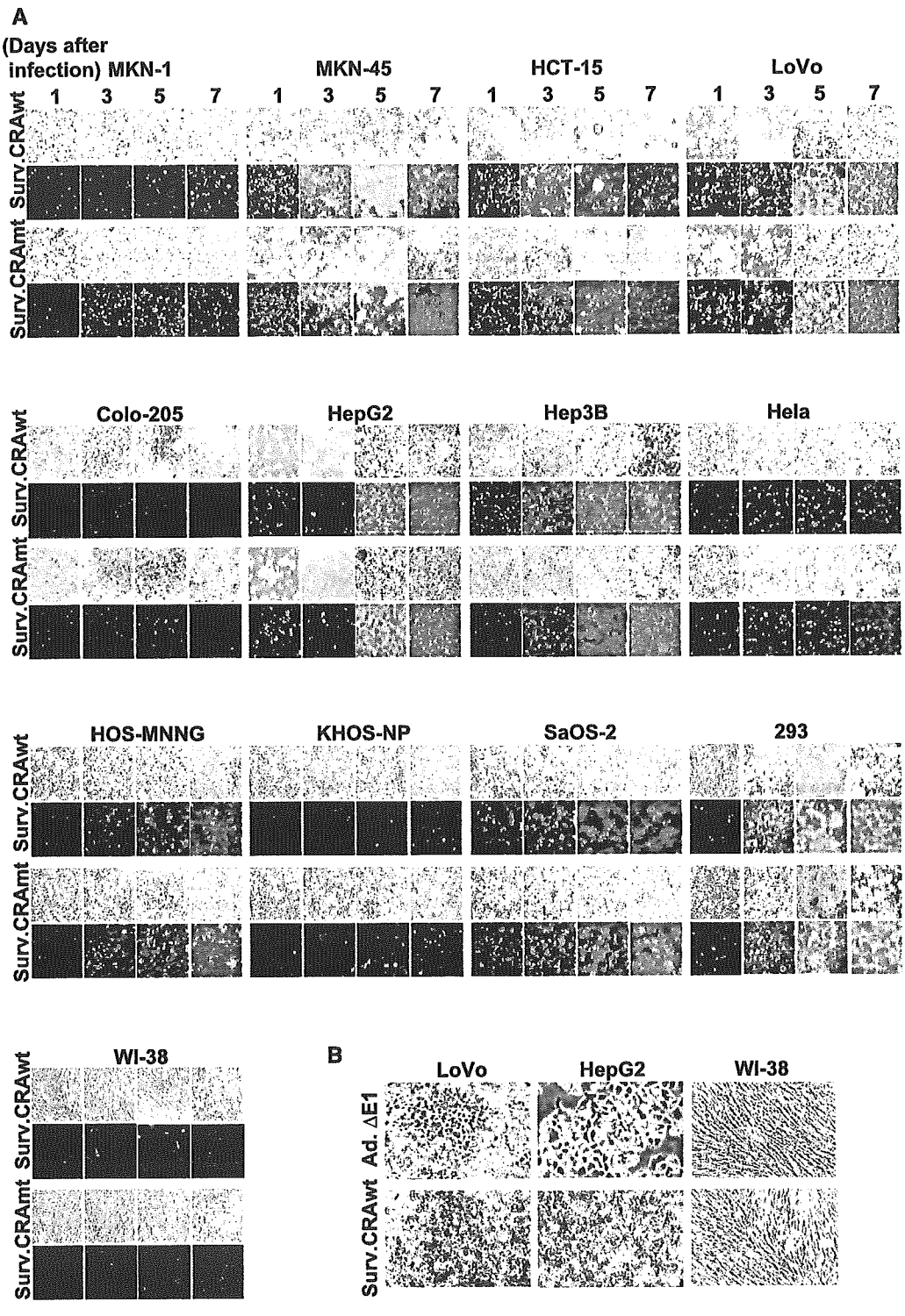

Figure 2. Replication and cytotoxicity of Surv.CRAs in different cell lines. *A*, representative phase-contrast (*top*) and fluorescent microscopic images (*bottom*) 1, 3, 5, and 7 days after infection with Surv.CRAwt or Surv.CRAmt at an MOI of 0.1. EGFP-positive cells increased in a time-dependent manner after infection with either Surv.CRAwt or Surv.CRAmt in all cancer cells examined; in contrast, no significant increases in EGFP-positive cells were observed in normal WI-38 cells. The rate of spreading of EGFP-positive cells and CPE correlated well with the endogenous levels of expression of *surivin* and the AGTE levels, as shown in Fig. 1. *B*, a high-power phase-contrast microscopic image taken 7 days after infection with control Ad.ΔE1 or Surv.CRAwt showed that all of the LoVo and HepG2 cells underwent cytopathic effect after infection with Surv.CRAwt only. In contrast, no cytopathic effect was observed in WI-38 cells after infection with either adenovirus.